Sea ice processes in Antarctic polynyas

Kenneth M. Golden

Department of Mathematics
University of Utah

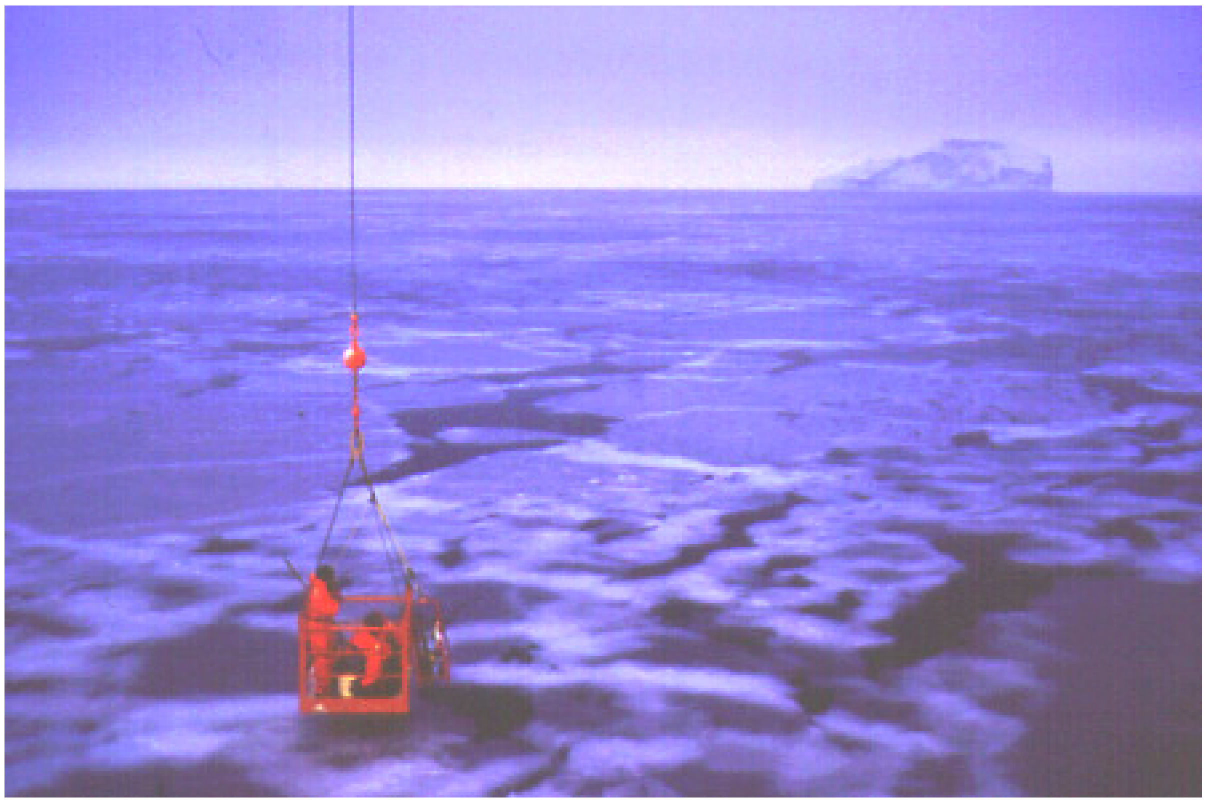

Mertz Glacier Polynya, July 1999

AIMS Orlando 1 July 2012

ANTARCTICA

southern cryosphere

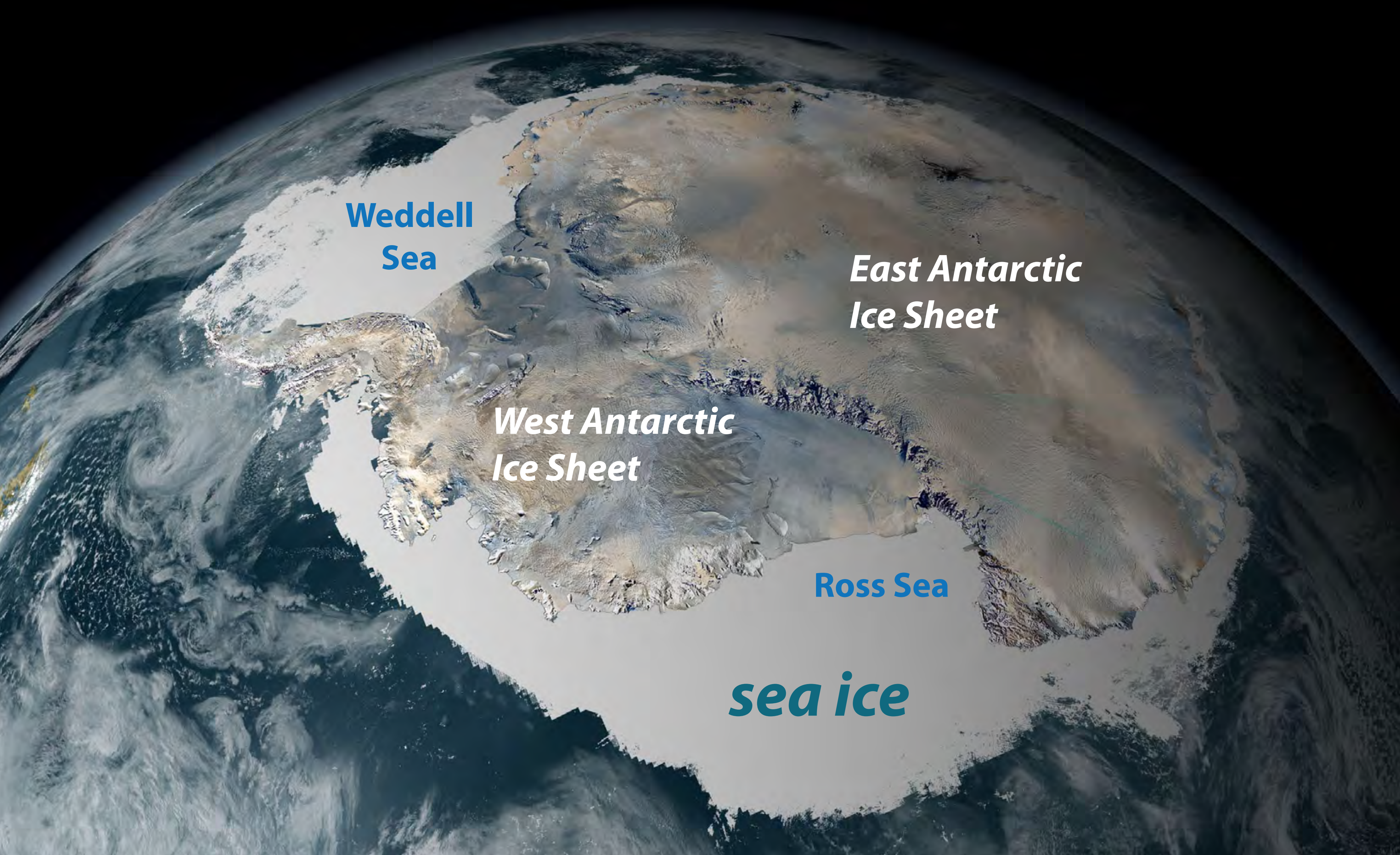

Polynyas

Size: 100 m - 1000 km

Two mechanisms can contribute to keeping polynyas open:

1. **Latent heat (or coastal) polynyas:** Mertz Glacier Polynya
   Sea ice grows in open-water and is continually removed by winds and currents (e.g. katabatic winds)
   - latent heat released to the ocean during ice formation perpetuates the process

2. **Sensible heat (or open-ocean) polynyas:** Weddell Polynya
   Upwelling warm waters, vertical heat diffusion, or convection may provide enough oceanic heat flux to maintain ice-free region

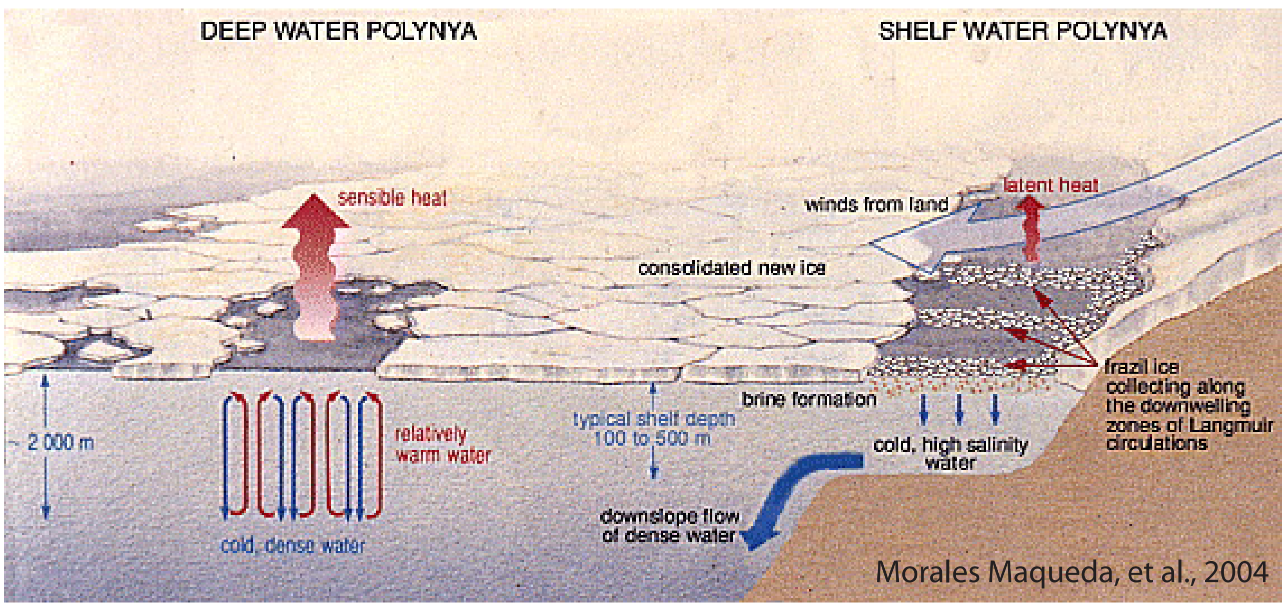

Antarctic coastal polynyas = ice factories

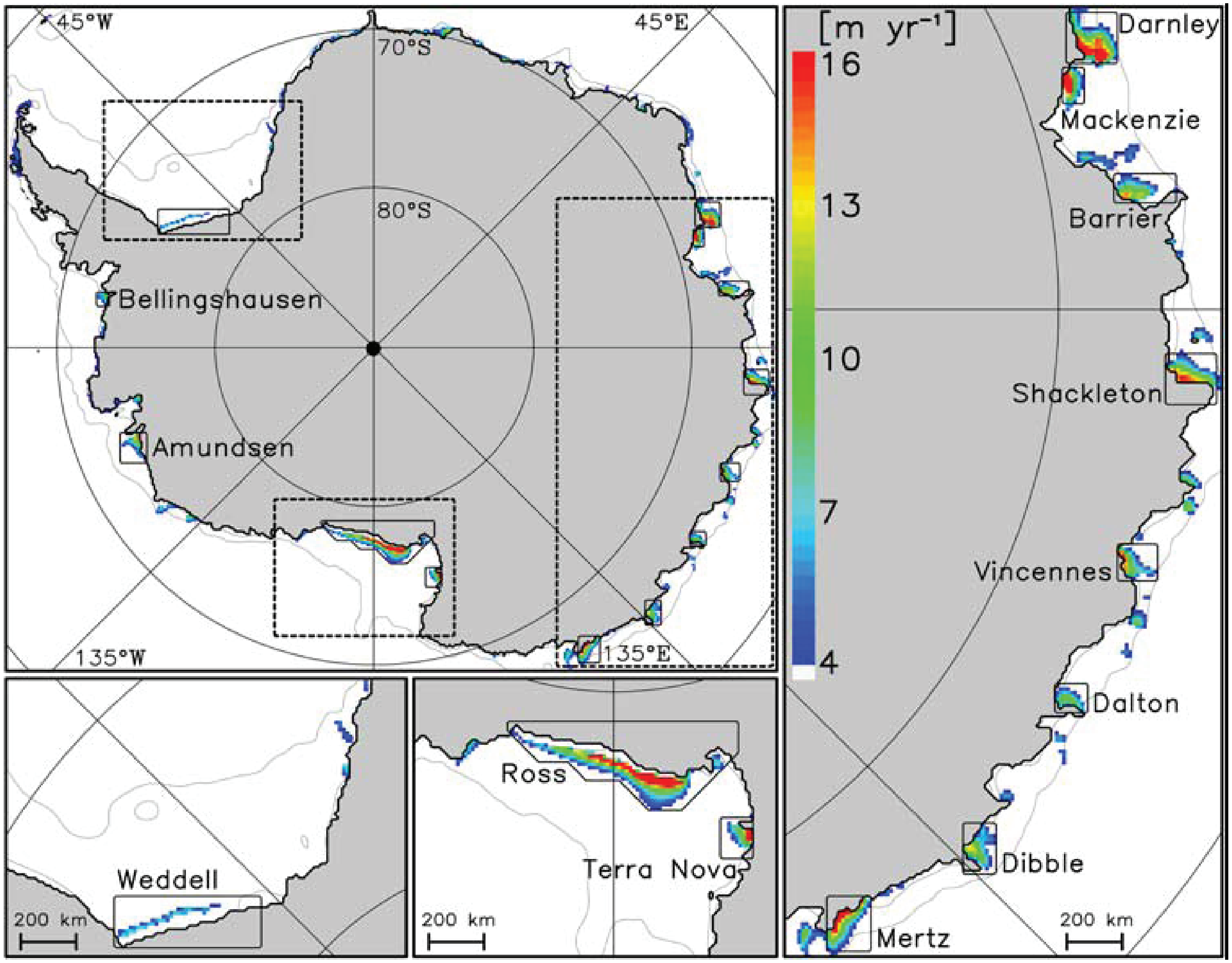

around 10% of Southern Ocean sea ice is produced in the major Antarctic coastal polynyas

ice production in Ross Ice Shelf Polynya decreased by about 30% from the 1990's to the 2000's

(caused by atmospheric warming or decreased polynya size from calving icebergs)

candidate for causing recent freshening of AABW

Tamura, Ohshima, Nihashi, GRL 2008

polynyas ice factories

Mertz Glacier Polynya, located in East Antarctica, covers only 0.001% of the overall Antarctic sea ice zone at its maximum winter extent, but is responsible for 1% of the total sea ice production in the Southern Ocean.

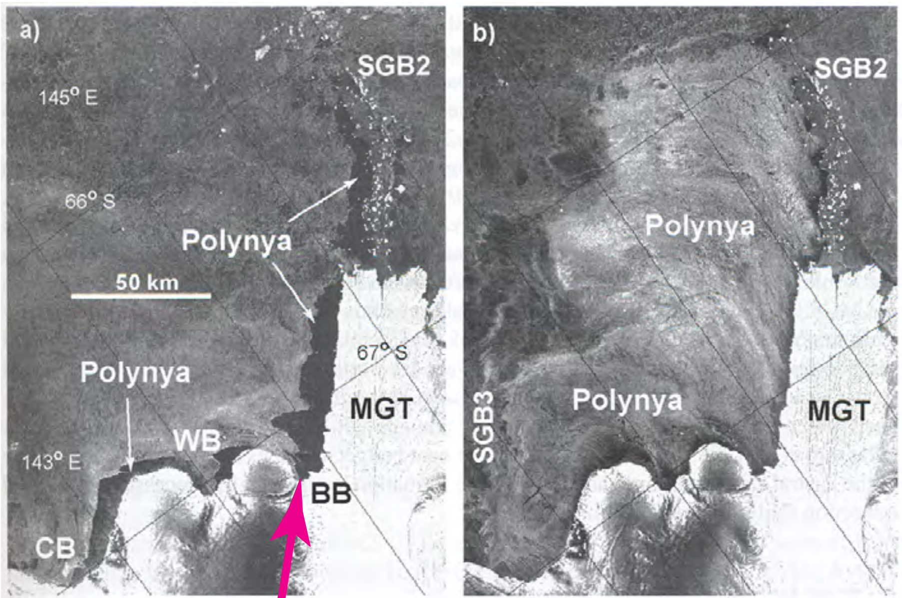

Buchanan Bay

Mertz Glacier Polynya -- third largest Antarctic sea ice producer

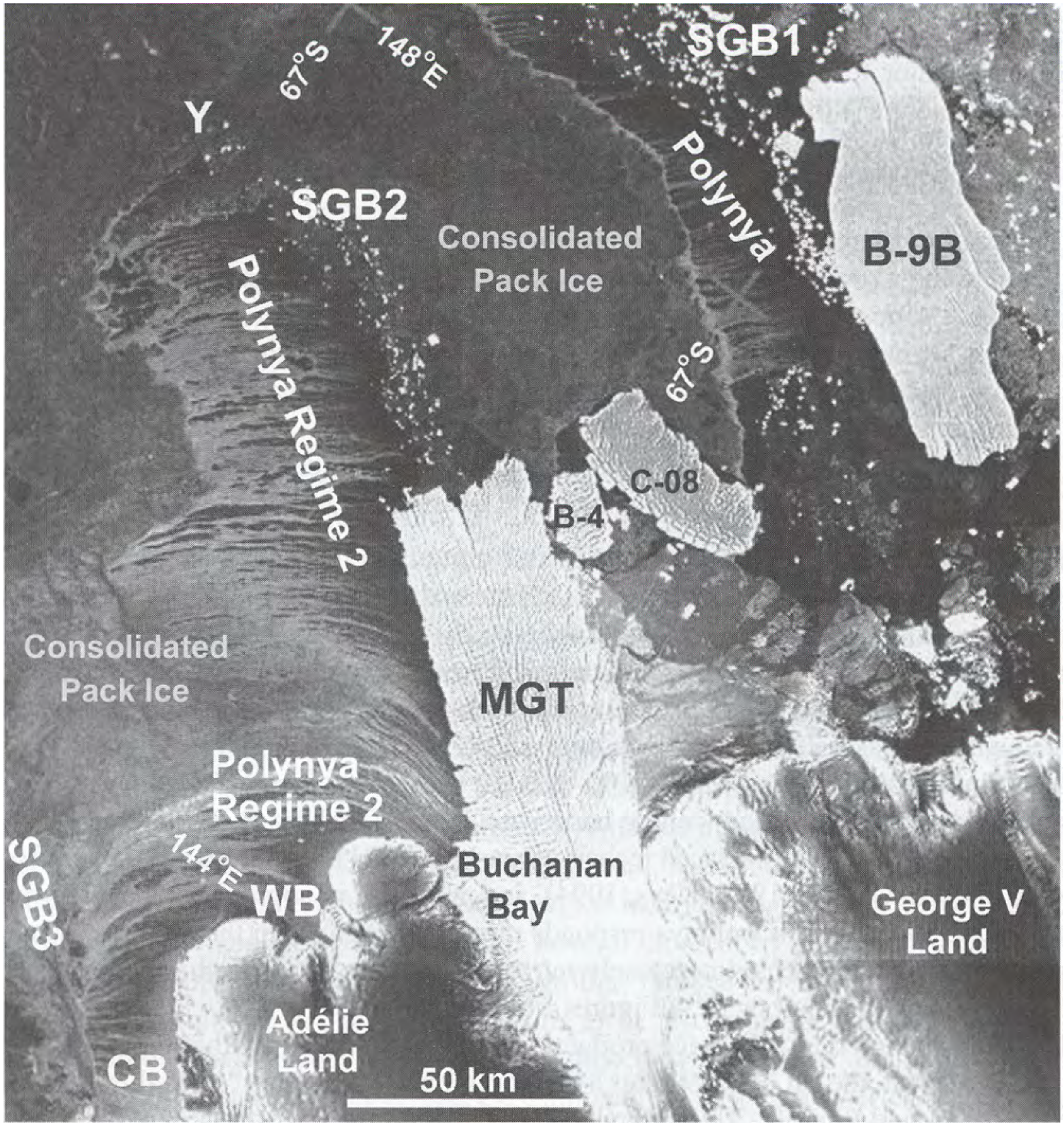

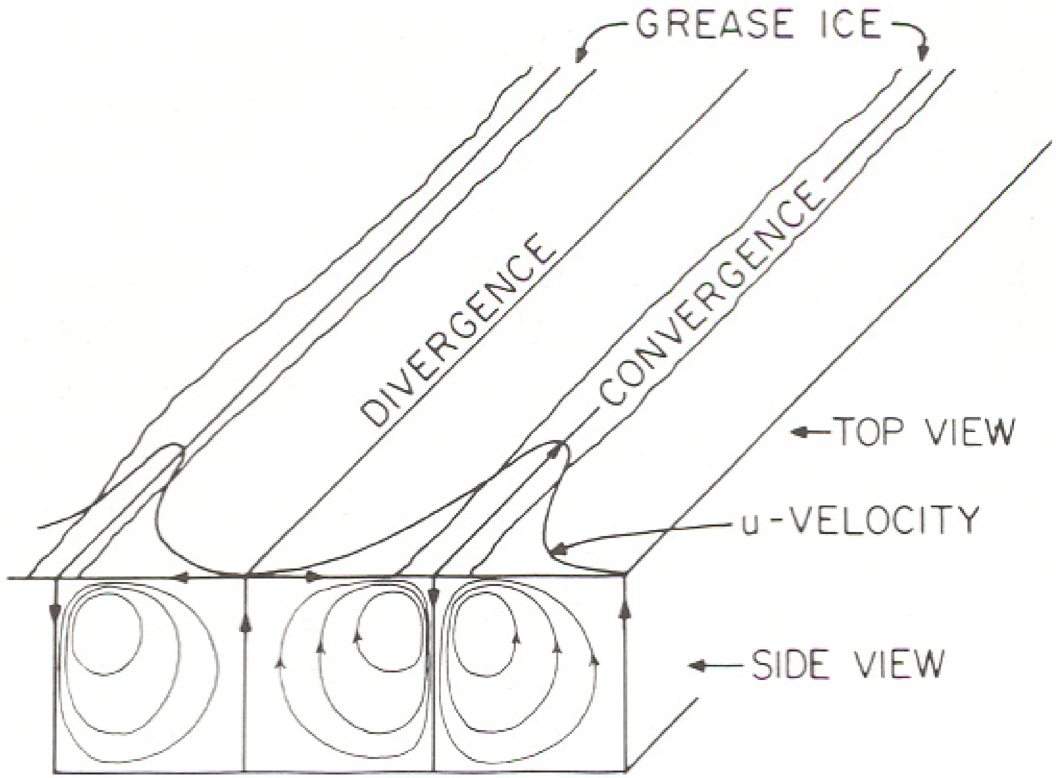

effect of Langmuir circulation
on grease and pancake ice

Martin and Kauffman, 1981

pancake ice

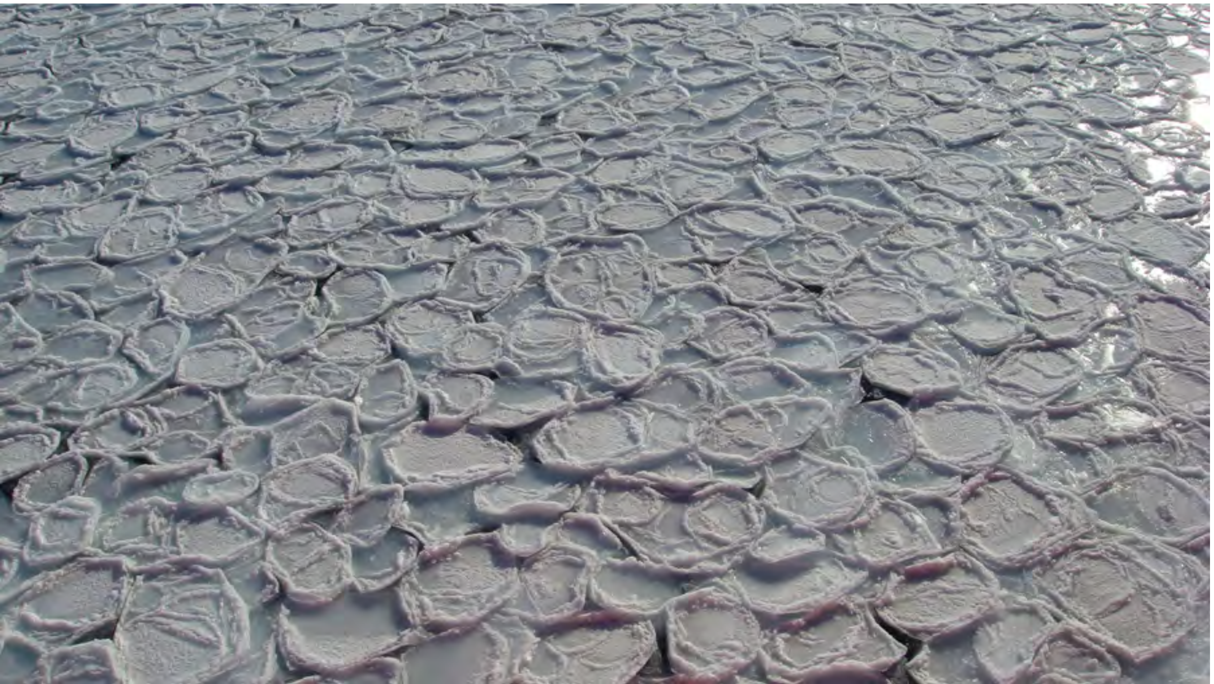

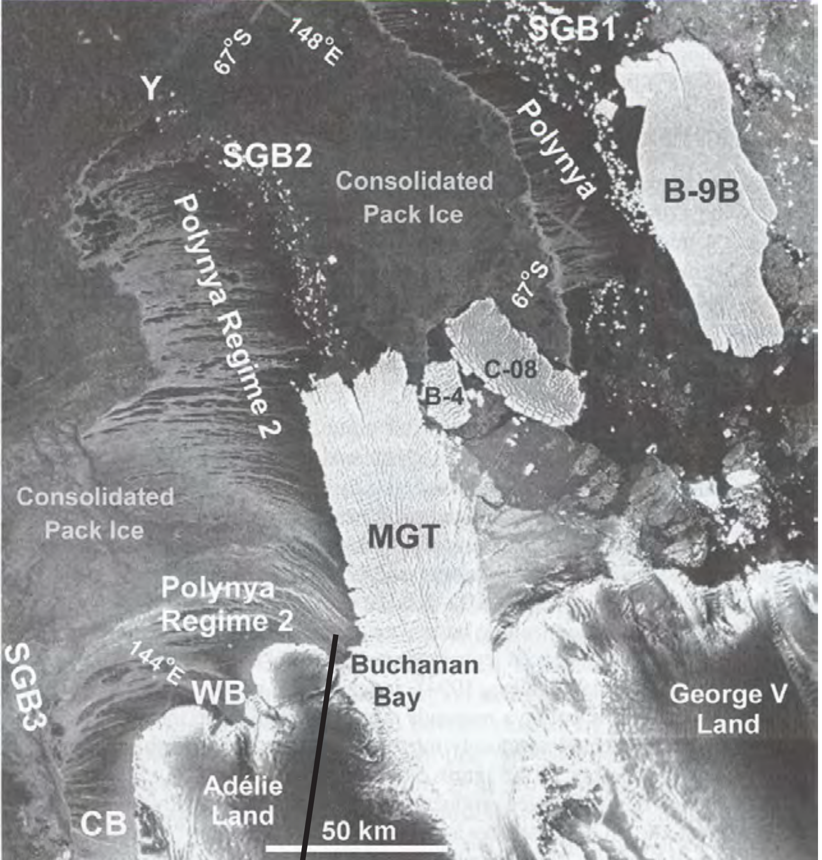
SGB1
Y
67°S
148°E
SGB2
Consolidated
Pack Ice
Polynya
B-9B
Polynya Regime 2
67°S
C-08
B-4
Consolidated
Pack Ice
MGT
Polynya
Regime 2
Buchanan
Bay
George V
Land
SGB3
144°E
WB
Adélie
Land
CB
50 km


iceberg collision!
breaking the Mertz Glacier Tongue, February 2010


Buchanan Bay, July 1999
Mertz Glacier Polynya Experiment

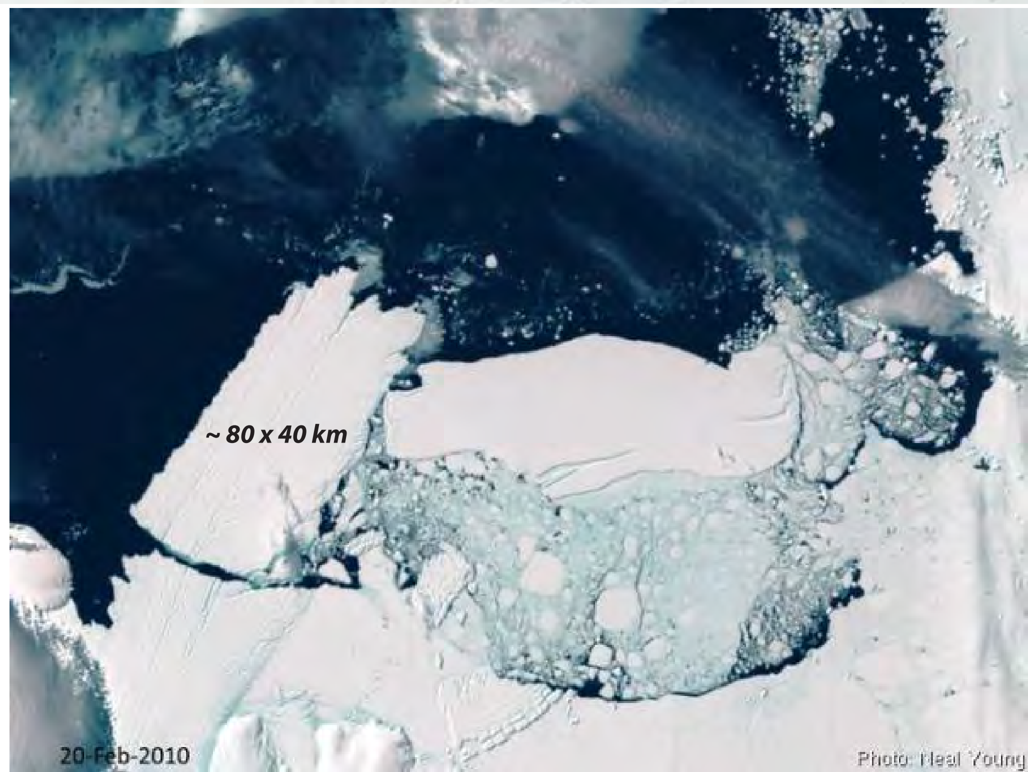
~ 80 x 40 km
20-Feb-2010
Photo: Neal Young

Weddell Polynya

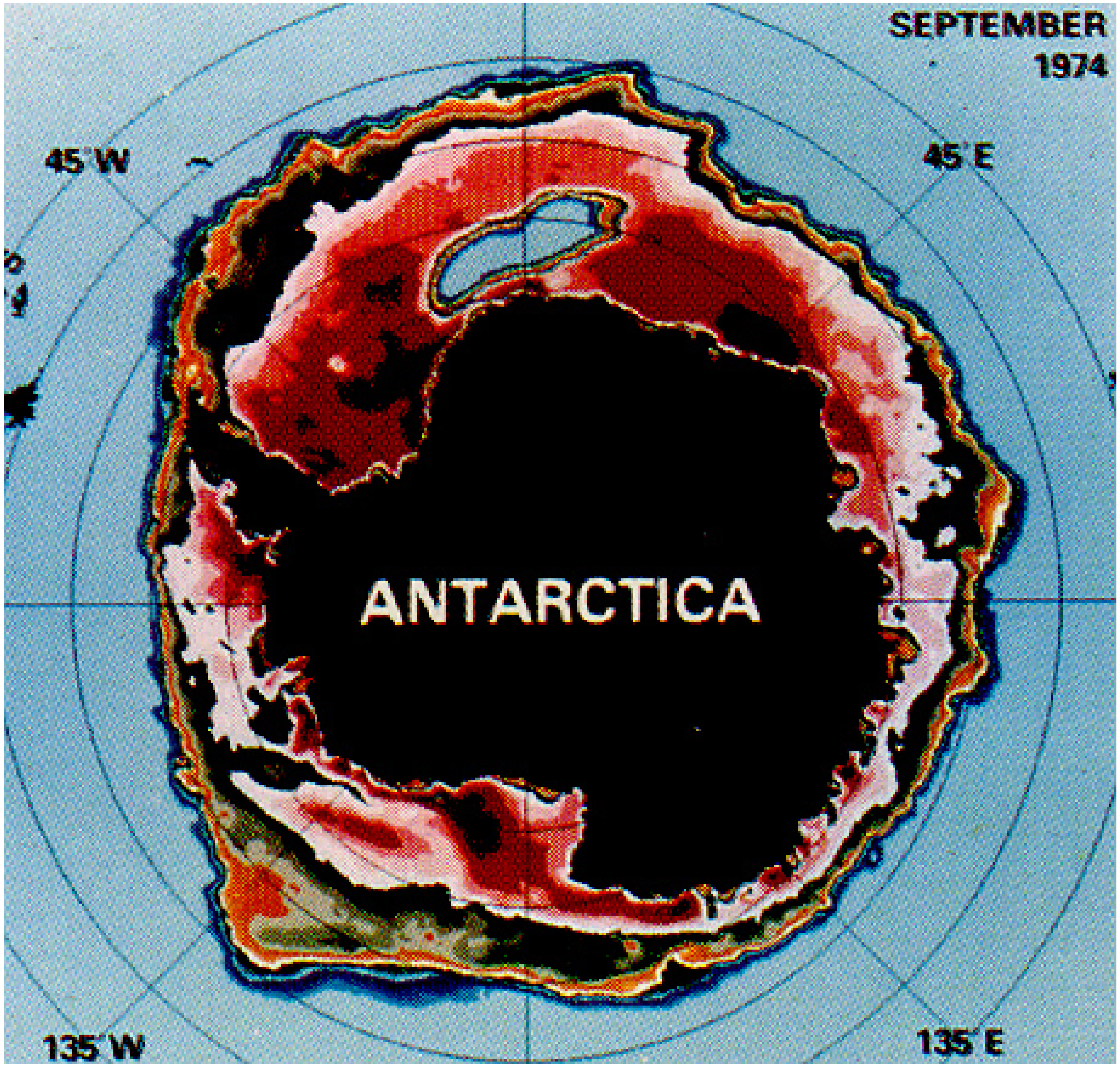

Antarctic Zone Flux Experiment (ANZFLUX) 1994

Antarctic Zone Flux Experiment
(ANZFLUX) 1994

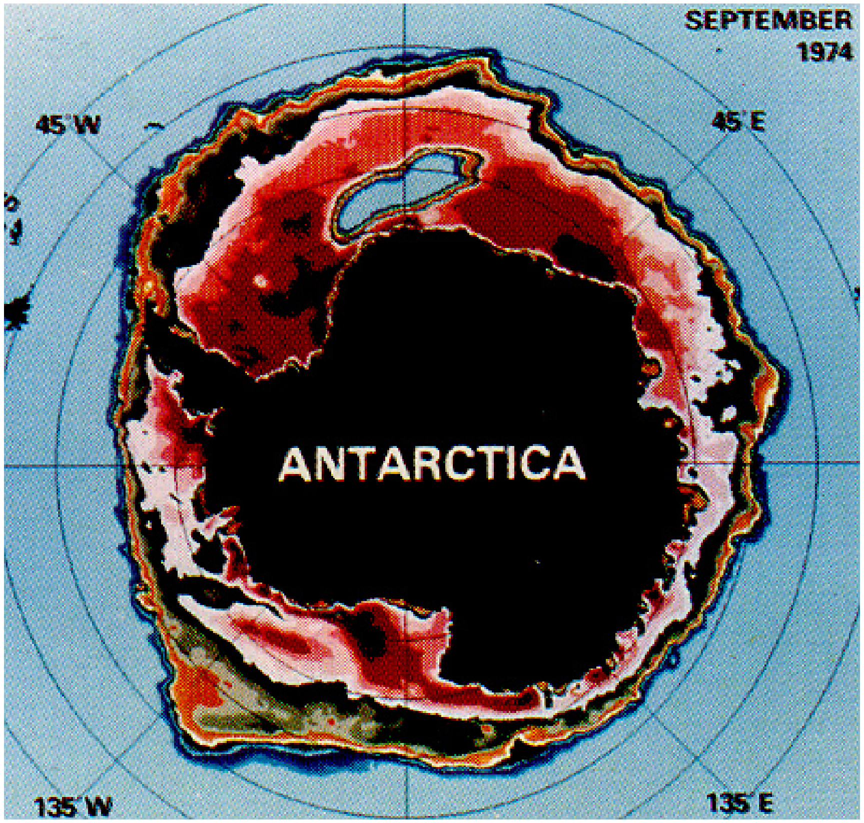

dynamic equilibrium of sea ice thickness

snow loading during storms

surface flooding ->
snow-ice formation

controlled by ice permeability

snow-ice growth a key process in Antarctic

may become more important in Arctic with
thinning ice and increased precipitation

Ackley, Lytle, Golden, Darling, Kuehn, 1995
Maksym and Jeffries, 2001

Maksym and Markus, 2008
Maksym and Golden, 2012

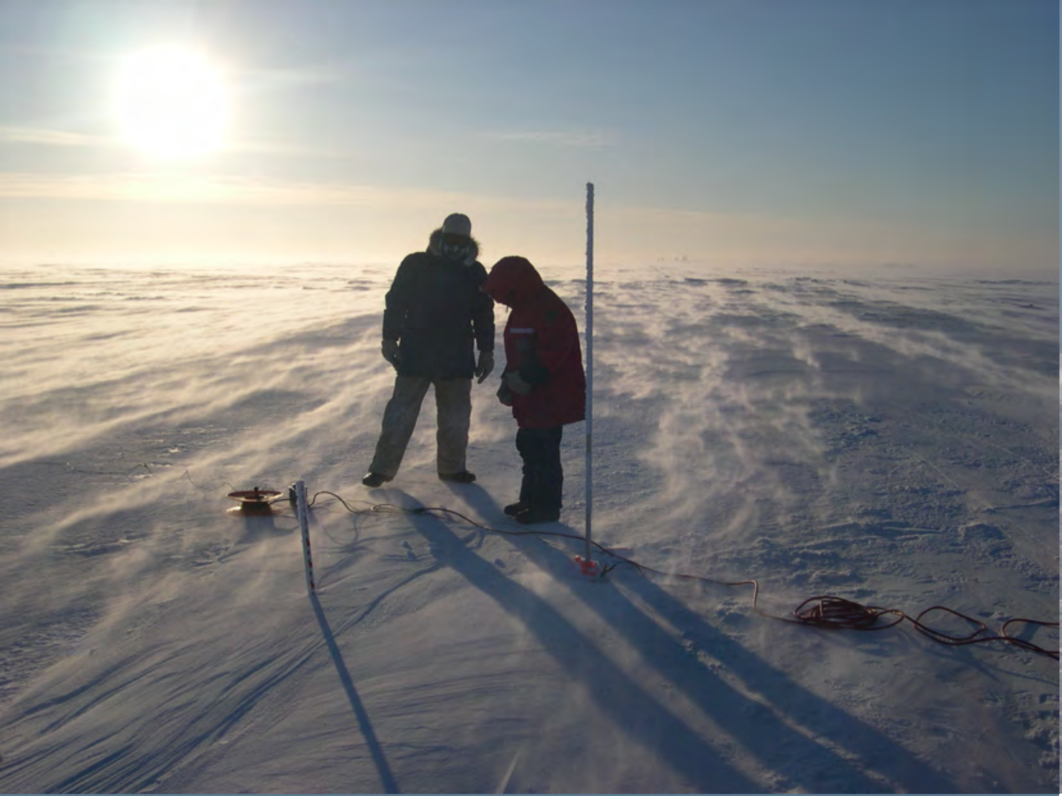

sea ice may appear to be a barren, impermeable cap ...

brine inclusions in sea ice (mm)

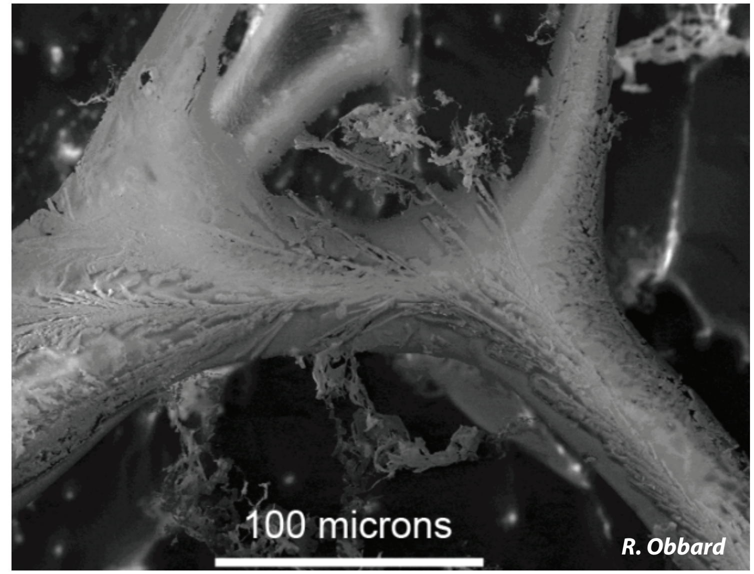

micro - brine channel (SEM)

brine channels (cm)

sea ice is a porous composite

pure ice with brine, air, and salt inclusions

horizontal section

vertical section

cross-sections of sea ice structure

$$T_{freeze} = -1.8^{\circ}\,\mathrm{C}$$

crystallographic texture

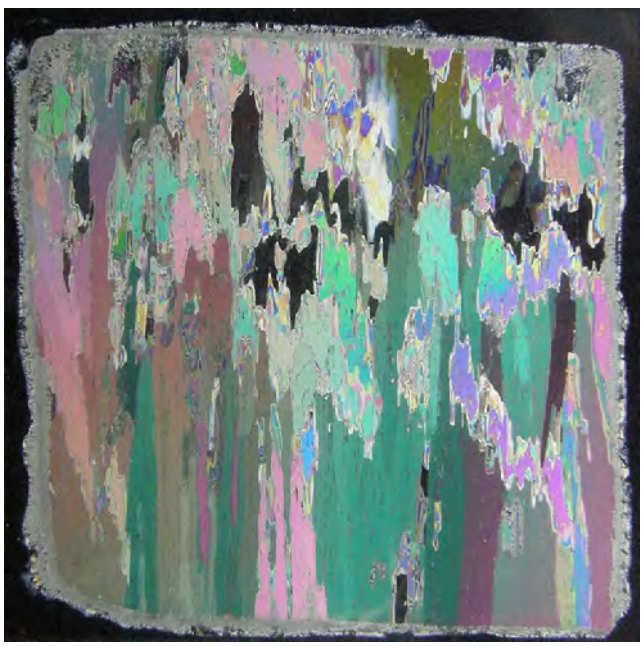

vertical thin section

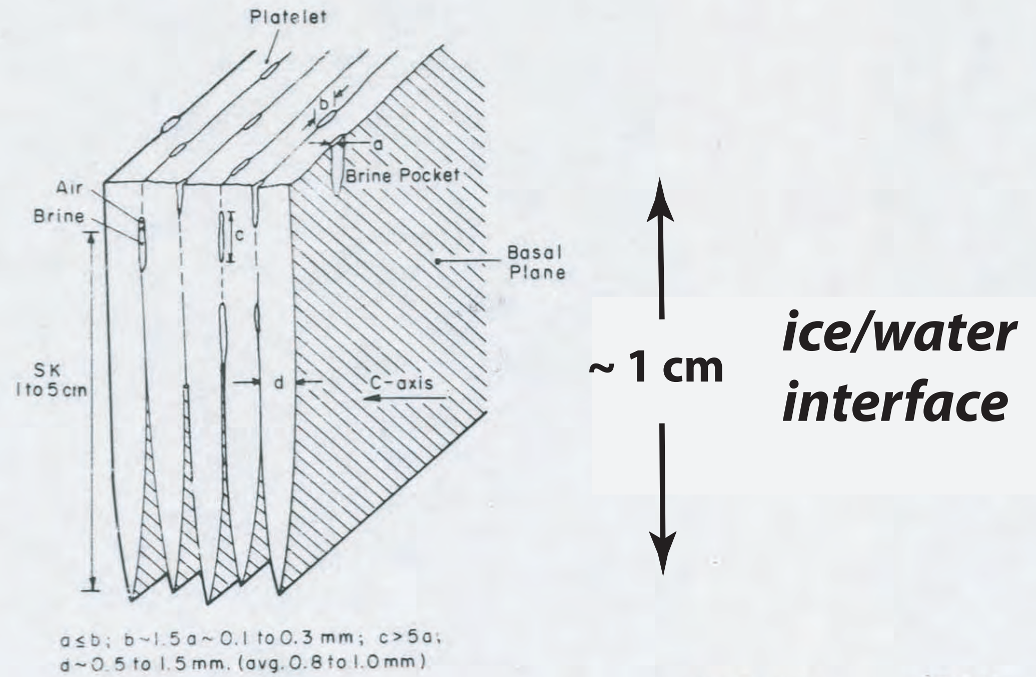

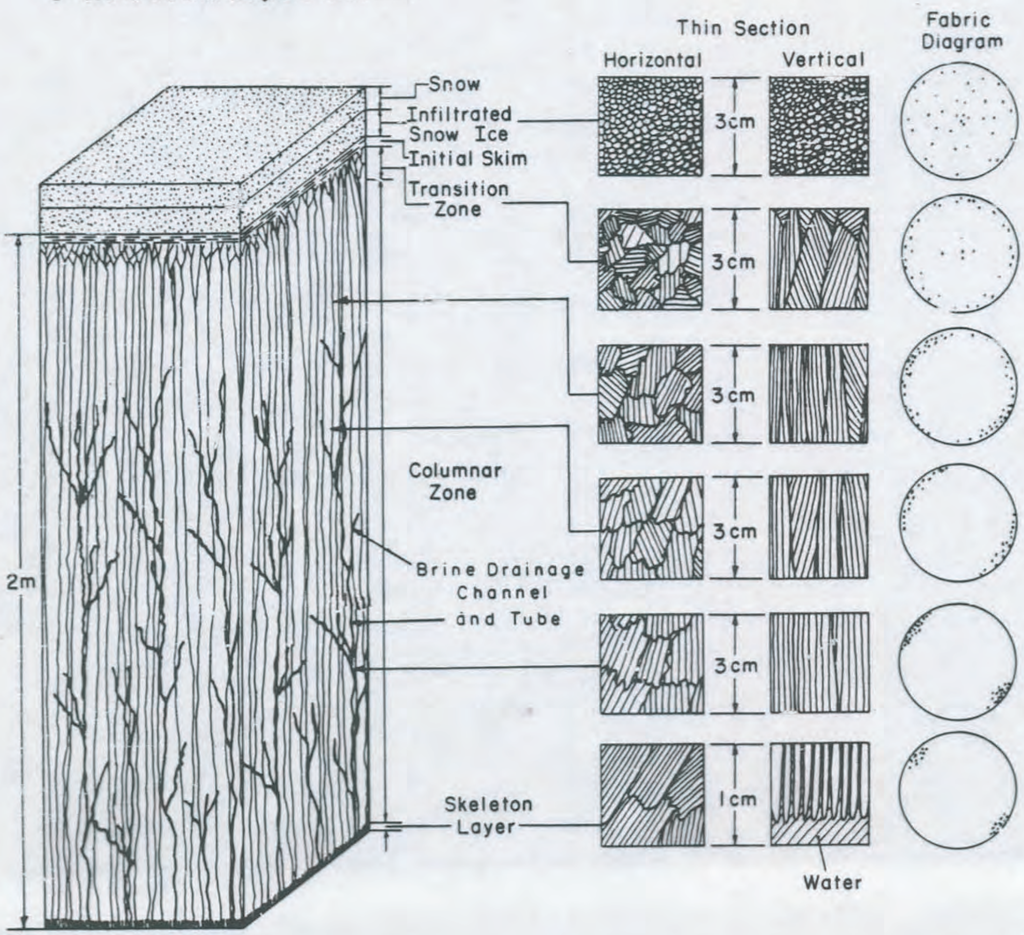

fluid flow through porous sea ice mediates key processes in polar climate and ecosystems:

evolution of Arctic melt ponds and sea ice albedo

nutrient flux for algal communities

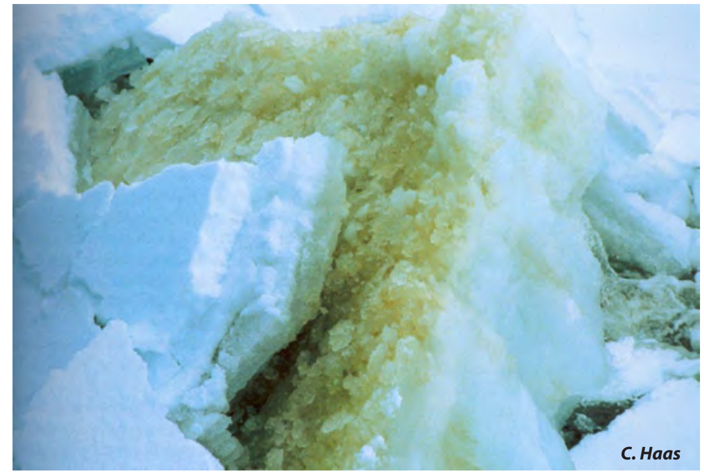

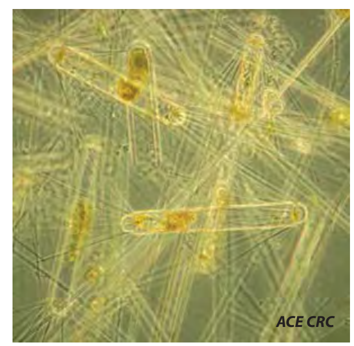

- *formation and melting of sea ice*
- *drainage of brine and melt water*
- *ocean-ice-atmosphere exchanges of heat, brine, CO2*
- *growth and decline of microbial communities*

Critical behavior of fluid transport in sea ice

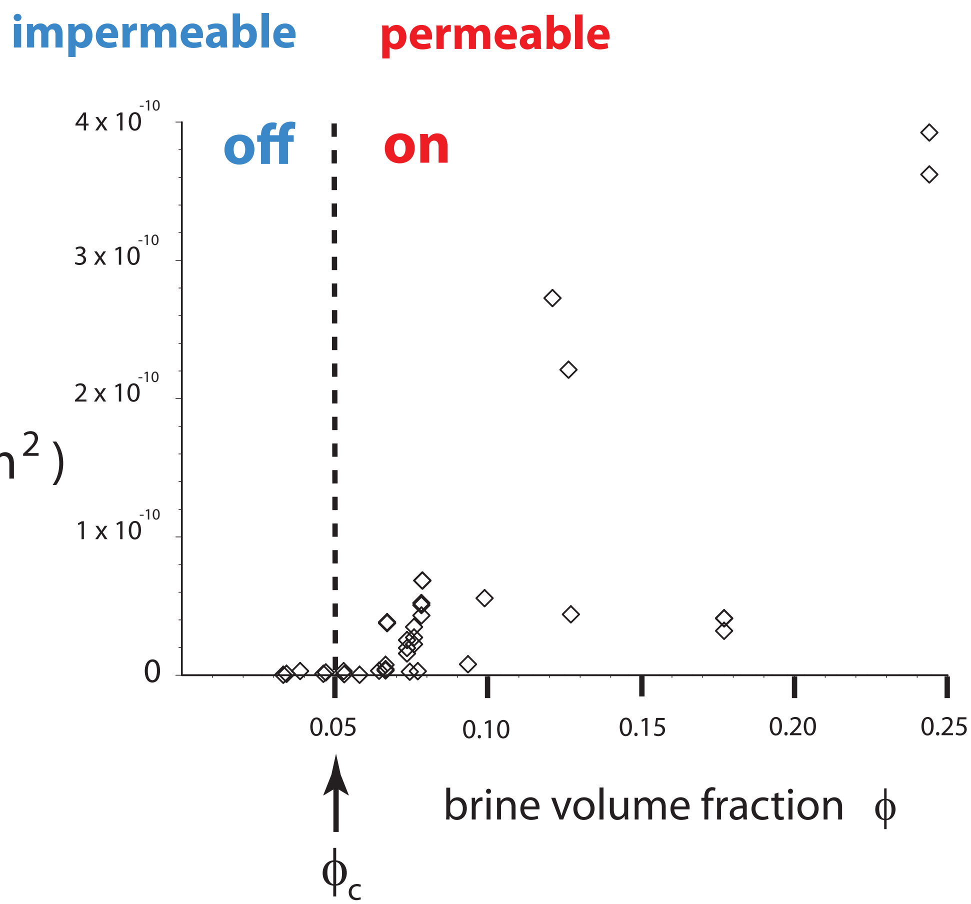

Arctic field data

vertical fluid permeability k (m^2)

"on - off" switch for fluid flow

critical brine volume fraction $\phi_c \approx 5\%$ $\longleftrightarrow$ $T_c \approx -5^\circ\mathrm{C}$, $S \approx 5$ ppt

RULE OF FIVES

Golden, Ackley, Lytle   Science   1998
Golden, Eicken, Heaton, Miner, Pringle, Zhu   Geophys. Res. Lett.   2007
Pringle, Miner, Eicken, Golden   J. Geophys. Res.   2009

rule of fives constrains:

Antarctic surface flooding and snow-ice formation

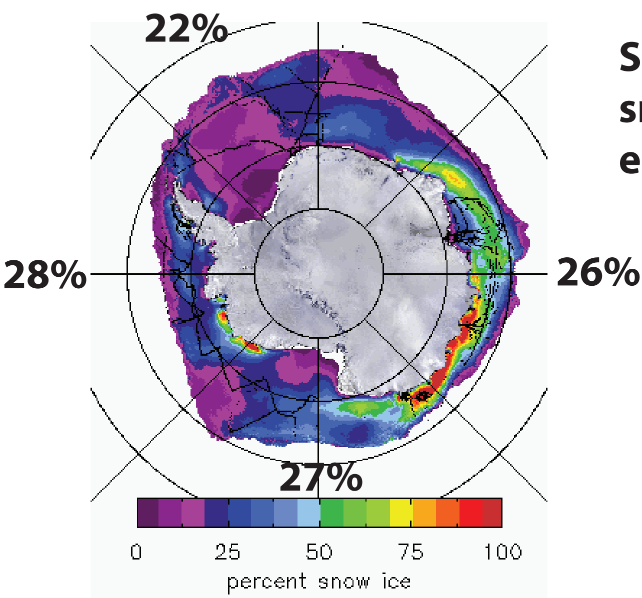

September snow-ice estimates

Antarctic snow-to-ice conversion from passive microwave imagery

T. Maksym and T. Markus, 2008

evolution of salinity profiles

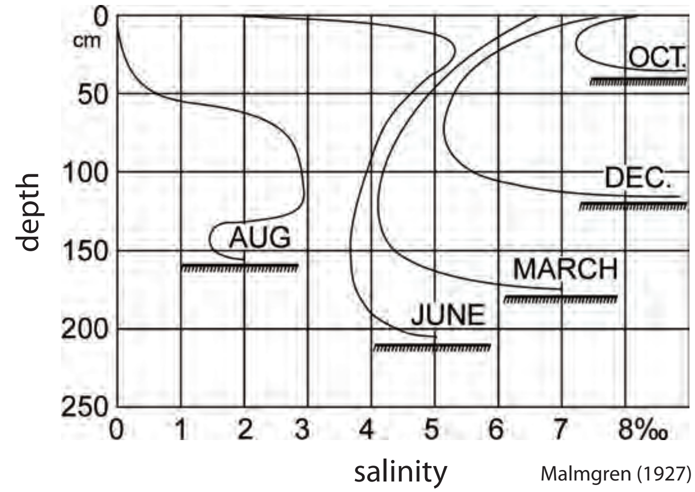

currently assumed constant in climate models

convection - enhanced thermal conductivity

Lytle and Ackley, 1996
Trodahl, et. al., 2000, 2001
Wang, Zhu, Golden, 2012

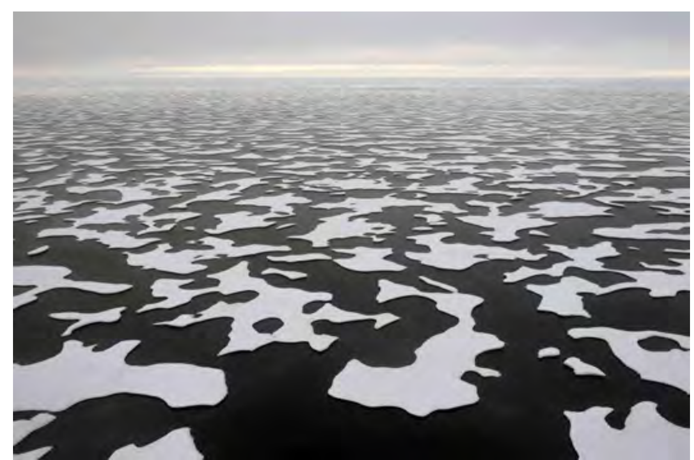

sea ice algal communities

D. Thomas 2004

nutrient replenishment controlled by ice permeability

biological activity turns on or off according to ***rule of fives***

critical behavior of microbial activity

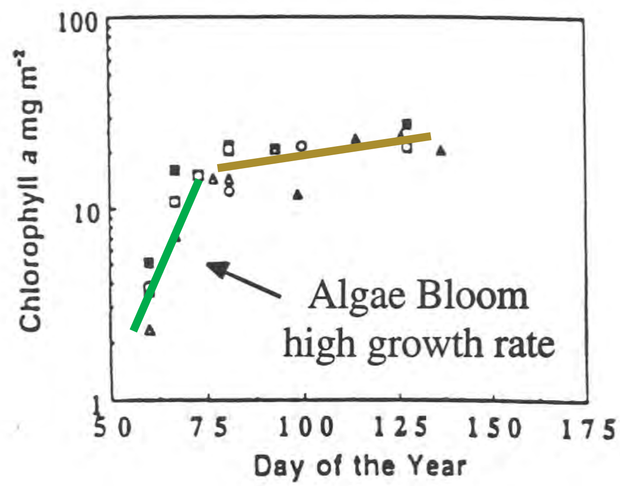

Convection-fueled algae bloom
Ice Station Weddell

Golden, Ackley, Lytle ***Science 1998***

Fritsen, Lytle, Ackley, Sullivan ***Science 1994***

ANZFLUX drift camp

snow loading, surface flooding and subsequent snow - ice formation

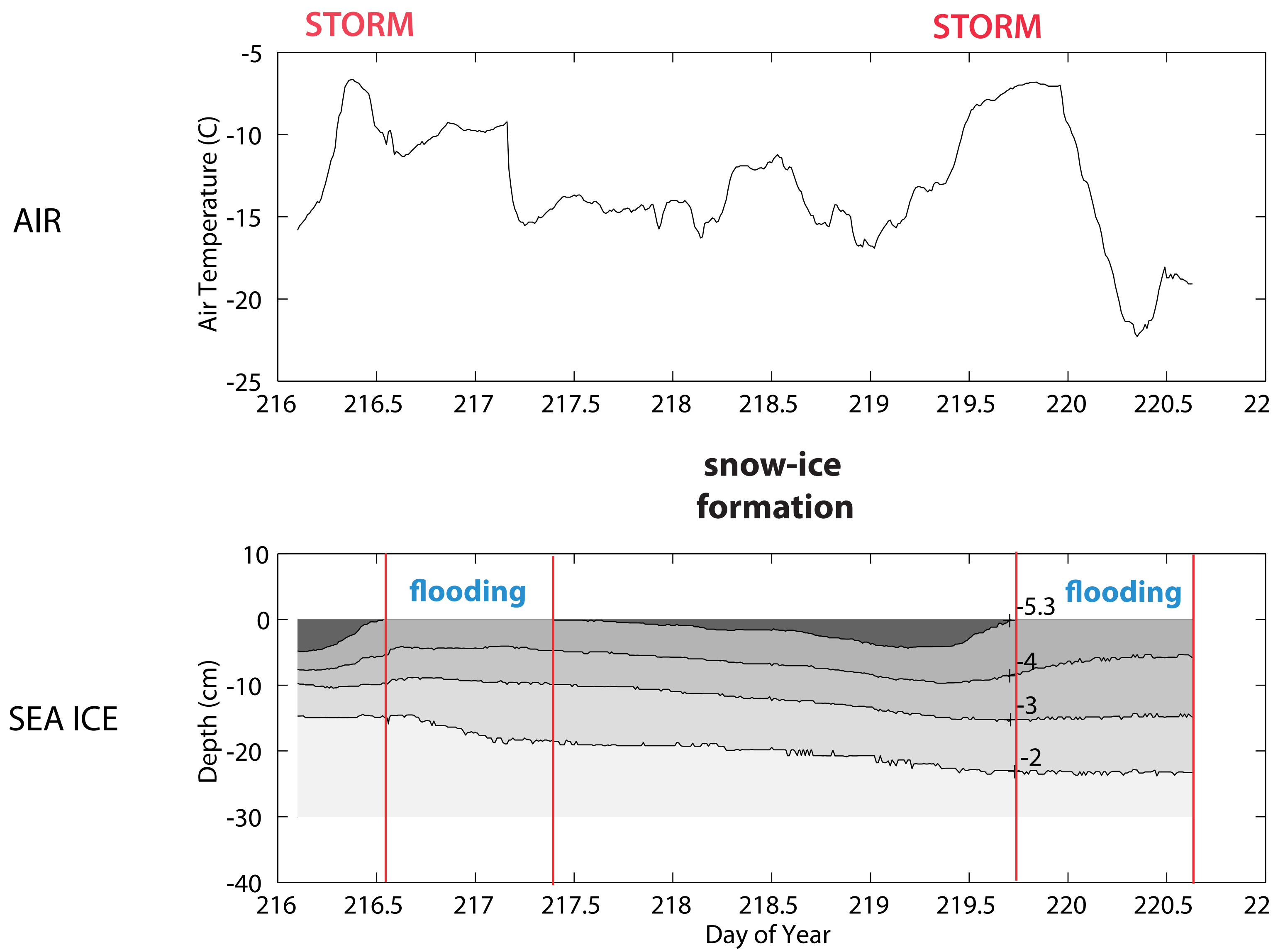

theoretical models explaining the *rule of fives* and fluid flow properties

percolation theory

mathematical theory of connectedness

impermeable

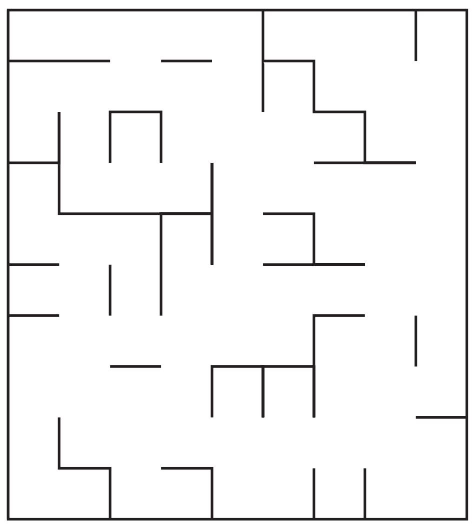

$p = 1/3$

permeable

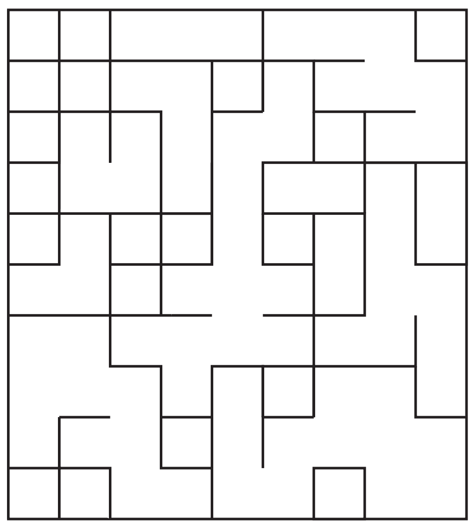

$p = 2/3$

a bond is open with probability p
closed with probability 1-p

percolation threshold

$p_c = 1/2 \quad \text{for} \quad d = 2$

first appearance of infinite cluster

order parameters in percolation theory

geometry

correlation length

characteristic scale
of connectedness

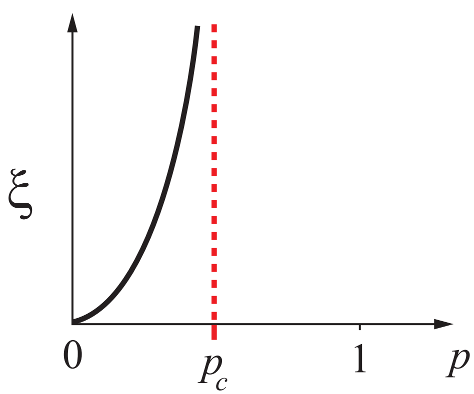

$$\xi\,(p) \sim |\,p - p_c|^{-\nu}$$

$$p \longrightarrow p_c$$

infinite cluster density

probability the origin
belongs to infinte cluster

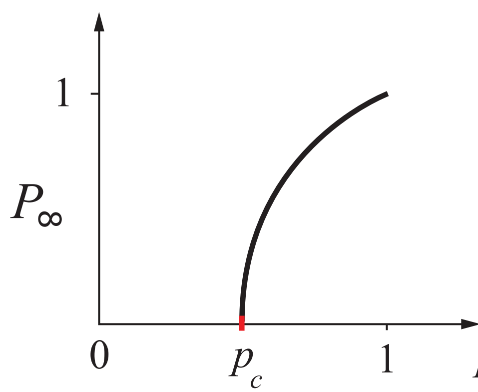

$$P_\infty(p) \sim (\,p - p_c)^{\beta}$$

$$p \longrightarrow p_c^+$$

transport

effective conductivity or fluid permeability

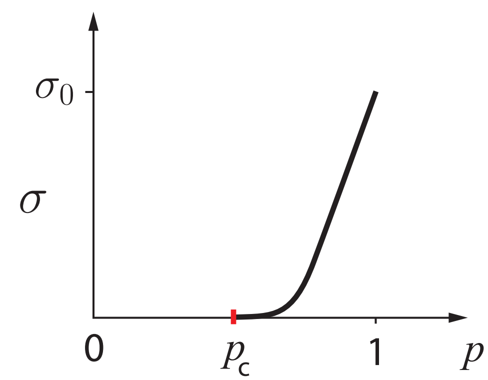

$$\sigma\,(p) \sim \sigma_0\,(p - p_c)^t$$

$$p \longrightarrow p_c^+$$

UNIVERSAL critical exponents for lattices -- depend only on dimension

(**$1 \leq t \leq 2$,** Golden, *Phys. Rev. Lett.* 1990 ; *Comm. Math. Phys.* 1992)

non-universal behavior in continuum

Continuum percolation model for stealthy materials applied to sea ice microstructure explains **Rule of Fives** and Antarctic data on ice production and algal growth

$\phi_c \approx 5\ \%$ Golden, Ackley, Lytle, *Science,* 1998

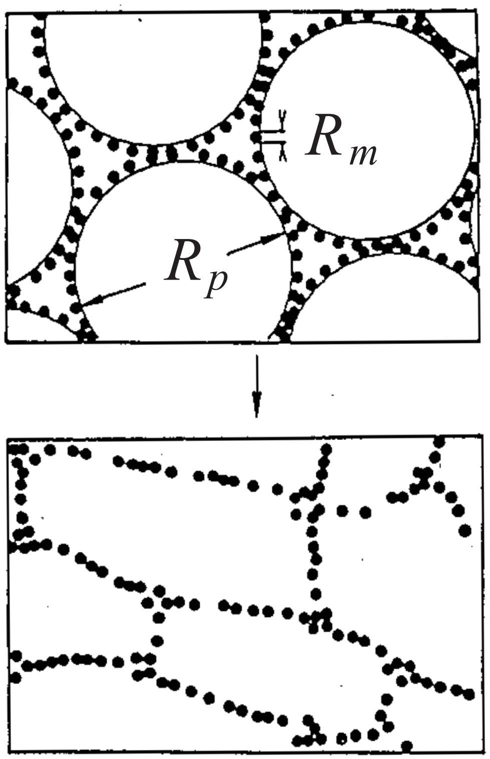

compressed powder

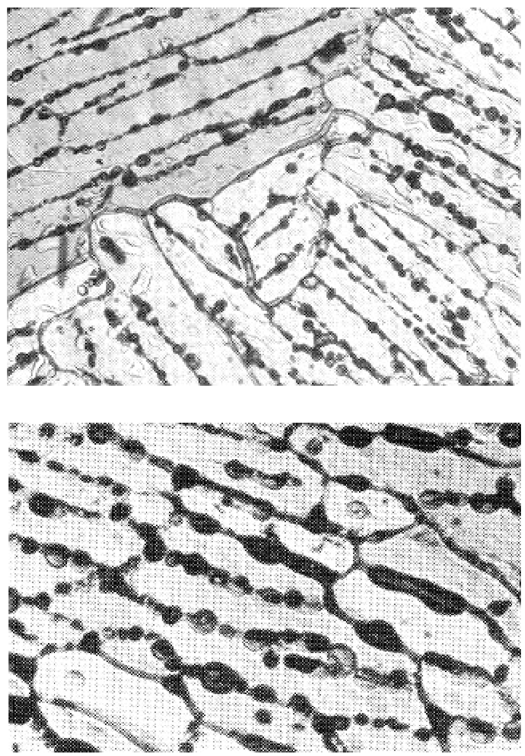

sea ice

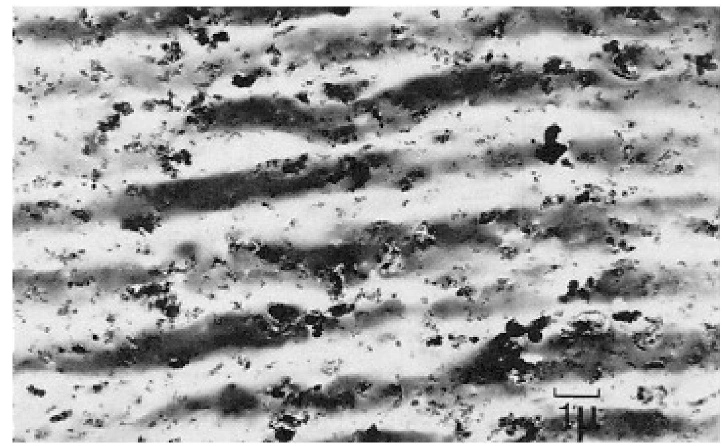

microstructure of radar absorbing composite

Thermal evolution of permeability and microstructure in sea ice **Golden, Eicken, Heaton, Miner, Pringle, Zhu**

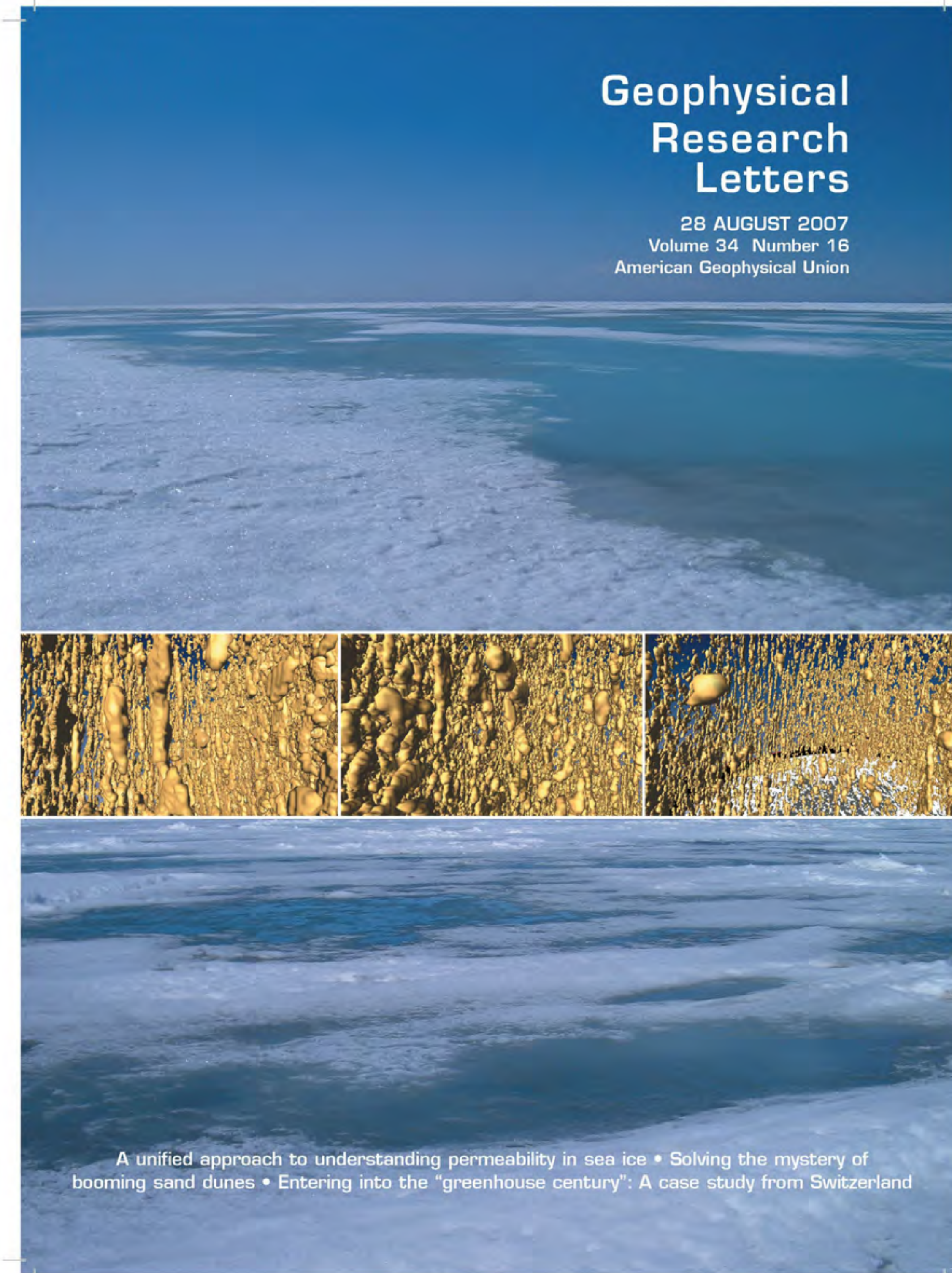

rigorous bounds
percolation theory
hierarchical model
network model

field data

micro-scale

controls

macro-scale processes

X-ray tomography for brine inclusions

unprecedented look at thermal evolution of brine phase and its connectivity

X-ray computed tomography of brine inclusions in sea ice

~ 1 cm across

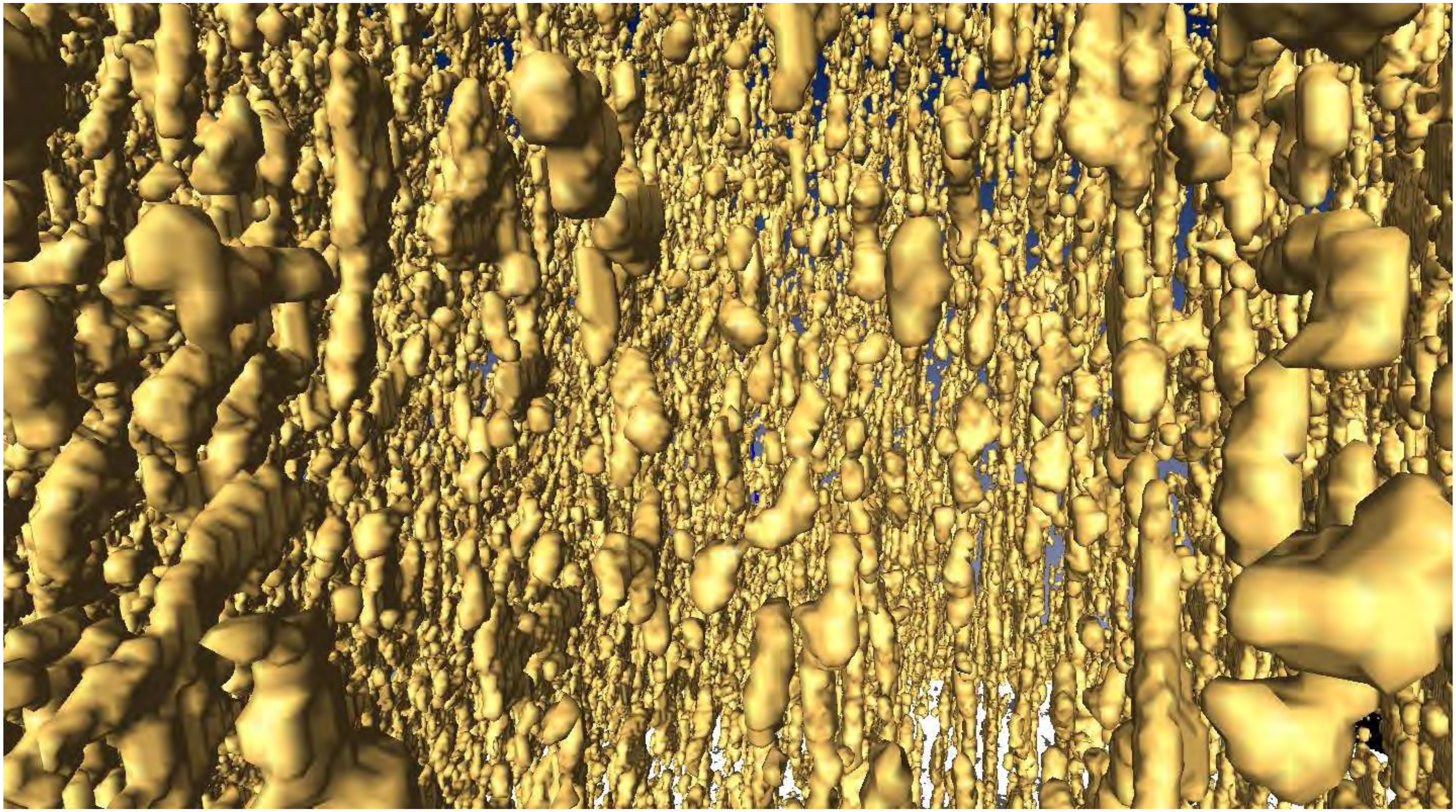

brine volume fraction $\phi = 5.7\ \%$ $T = -8^{\circ}C$

Golden, Eicken, Heaton, Miner, Pringle, Zhu, *Geophys. Res. Lett.* 2007

brine connectivity (over cm scale)

8 x 8 x 2 mm

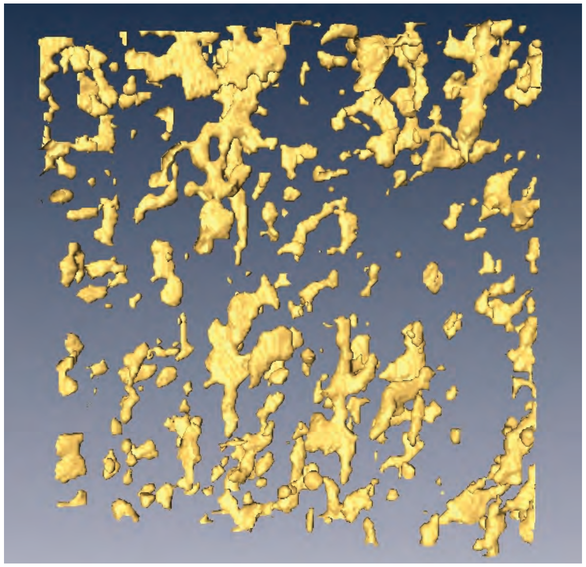

-15 °C, $\phi = 0.033$

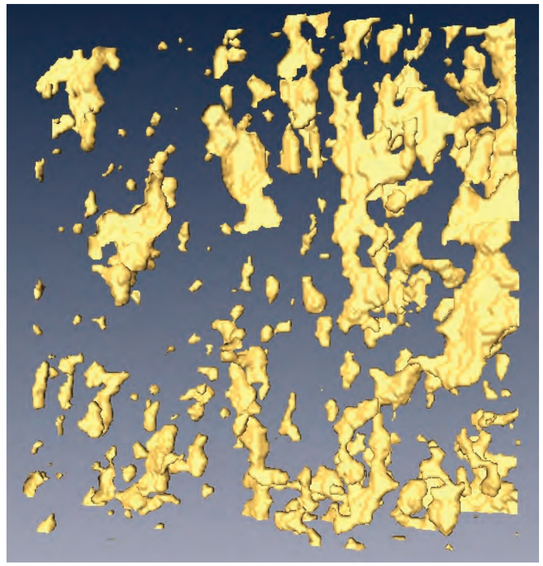

-6 °C, $\phi = 0.075$

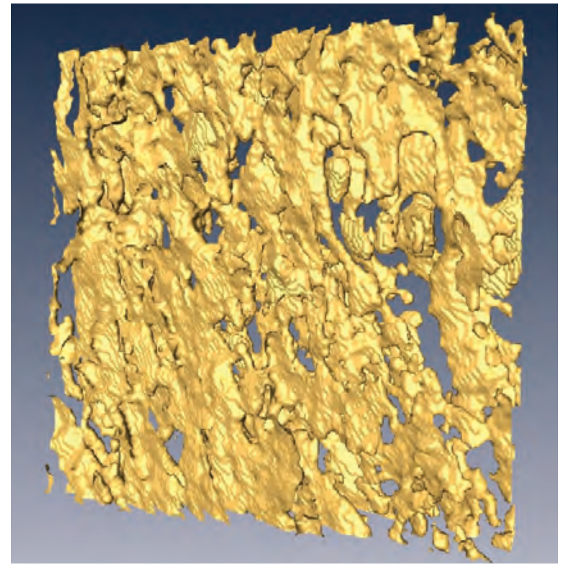

-3 °C, $\phi = 0.143$

X-ray tomography confirms percolation threshold

3-D images
pores and throats → 3-D graph
nodes and edges

analyze graph connectivity as function of temperature and sample size

- ***use finite size scaling techniques to confirm rule of fives***
- ***order parameter data from a natural material***

Pringle, Miner, Eicken, Golden, J. Geophys. Res. 2009

lattice and continuum percolation theories yield:

$$k(\phi) = k_0 (\phi - \phi_c)^2$$

critical
exponent
t

$$k_0 = 3 \text{ x } 10^{-8} \text{ m}^2$$

- exponent is UNIVERSAL lattice value $t \approx 2.0$ from general structure of brine inclusion distribution function (-- other saline ice?)

- sedimentary rocks like sandstones also exhibit universality

- critical path analysis -- developed for electronic hopping conduction -- yields scaling factor k_0

- no free parameters - microstructural input only

hierarchical and network models

brine-coated spherical ice grains

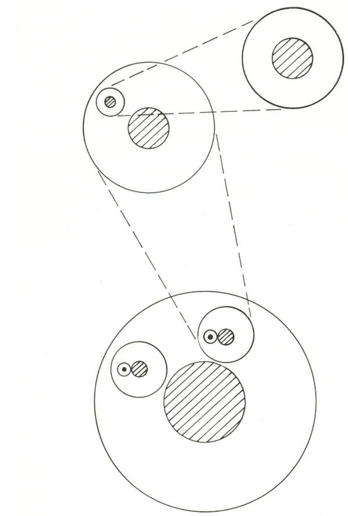

hierarchical model : $y = 3\,x - 7.5$

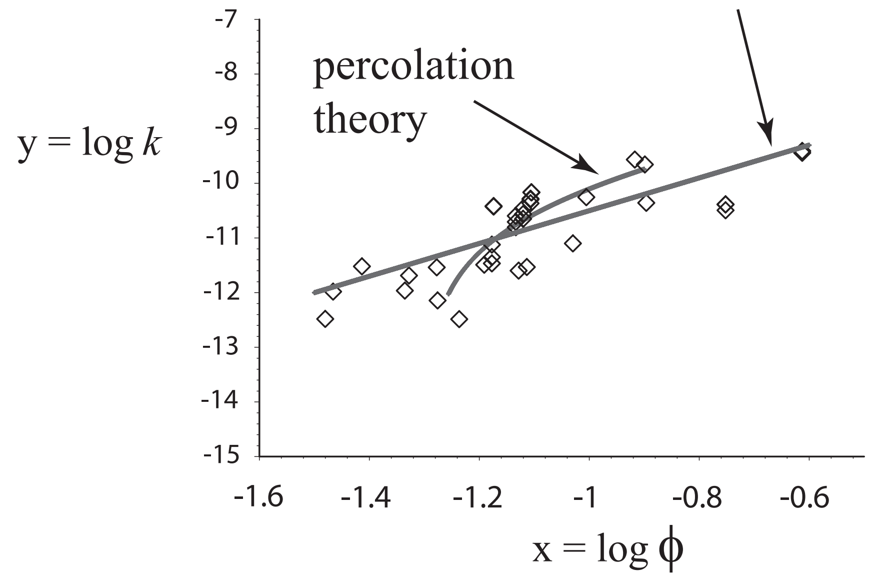

statistical best fit of data: $y = 3.05\,x - 7.50$

$$k\,(\phi) = k_0\,\phi^3$$

self-similar model used for porous rocks

Sen, Scala, Cohen 1981
Sheng 1990
Wong, Koplick, Tomanic 1984

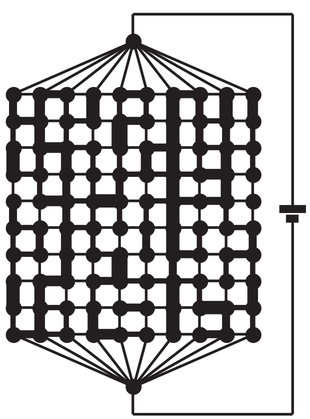

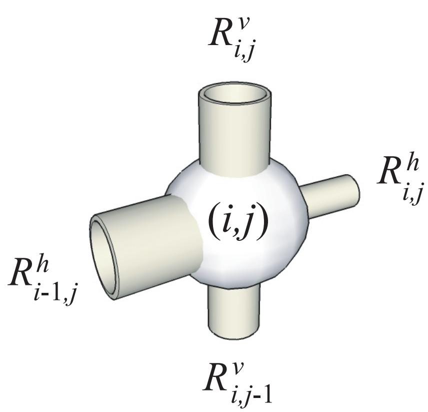

random pipe network with radii chosen from measured inclusion distributions, solved with fast multigrid method

Zhu, Jabini, Golden, Eicken, Morris, Annals of Glaciology, 2006
Golden et al., Geophysical Research Letters, 2007
Zhu, Golden, Gully and Sampson, Physica B, 2010

develop electromagnetic methods of monitoring fluid transport and microstructure

extensive measurements of fluid and electrical transport properties of sea ice:

2007	***Antarctic***	***SIPEX***
2010	***Arctic***	***Barrow AK***
2010	***Antarctic***	***McMurdo Sound***
2011	***Arctic***	***Barrow AK***
2012	***Arctic***	***Barrow AK***
2012	***Antarctic***	***SIPEX II***

electrical measurements

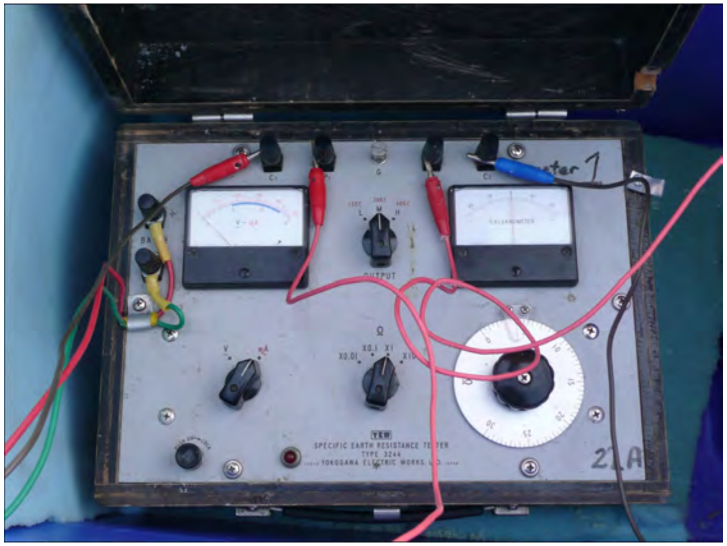

Wenner array

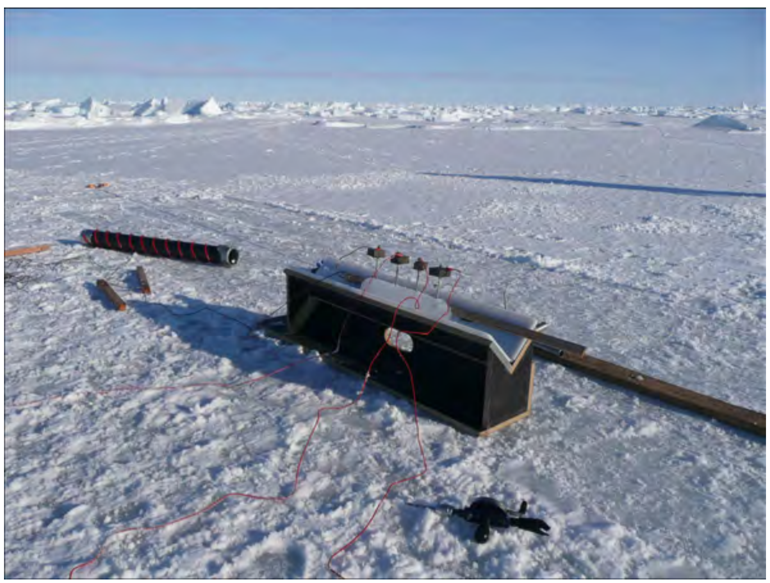

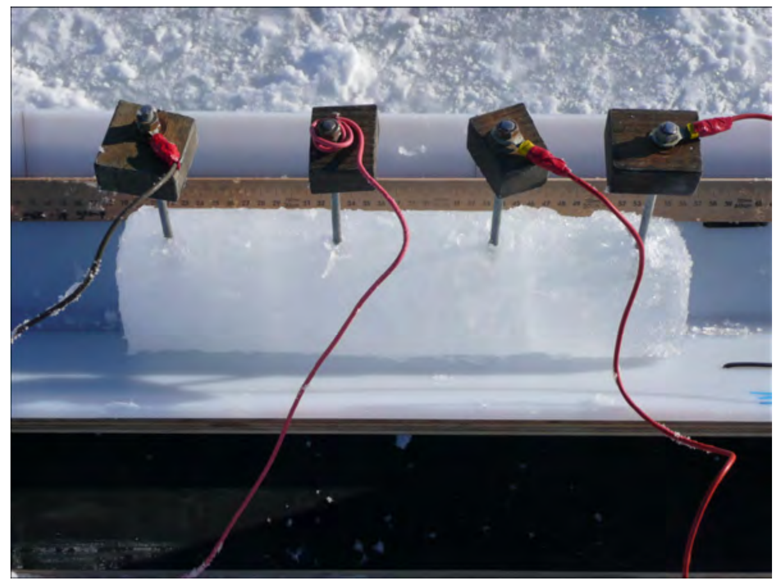

vertical conductivity

Zhu, Golden, Gully, Sampson ***Physica B*** 2010

Sampson, Golden, Gully, Worby ***Deep Sea Research*** 2011

critical behavior of electrical transport in sea ice

electrical signature of the on-off switch for fluid flow

same universal critical exponent as for fluid permeability

studied for over 50 years but no previous observations or theory of critical behavior

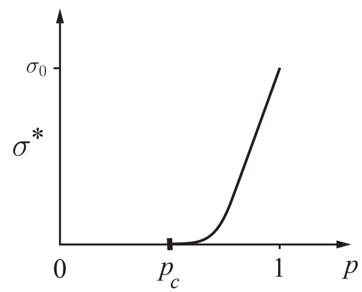

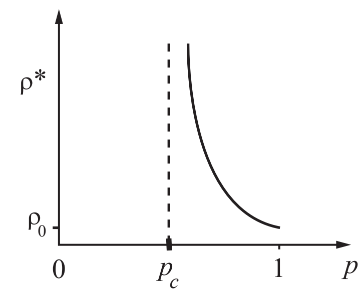

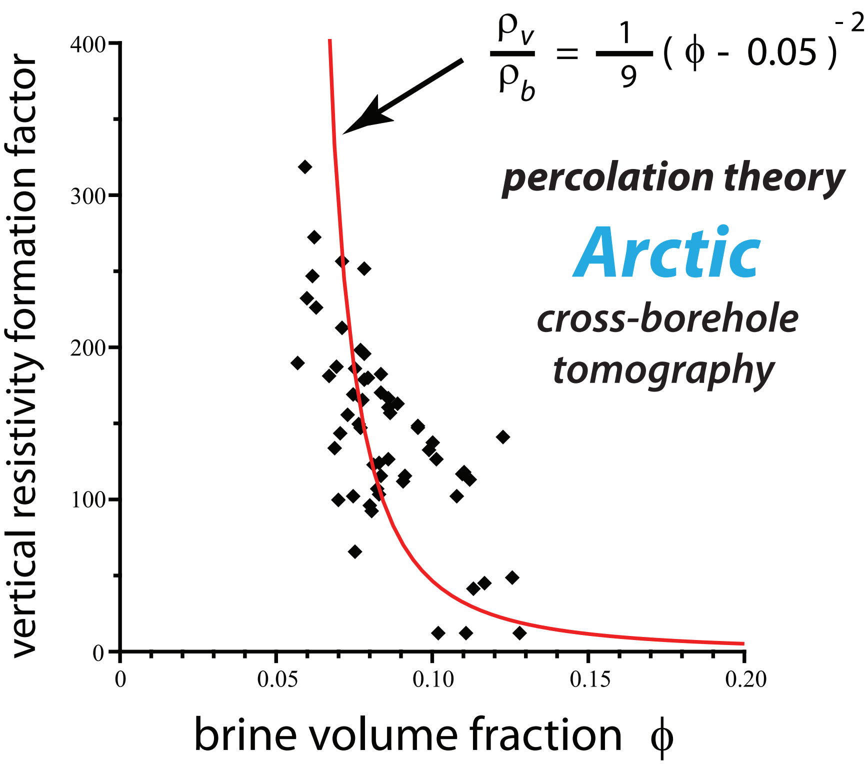

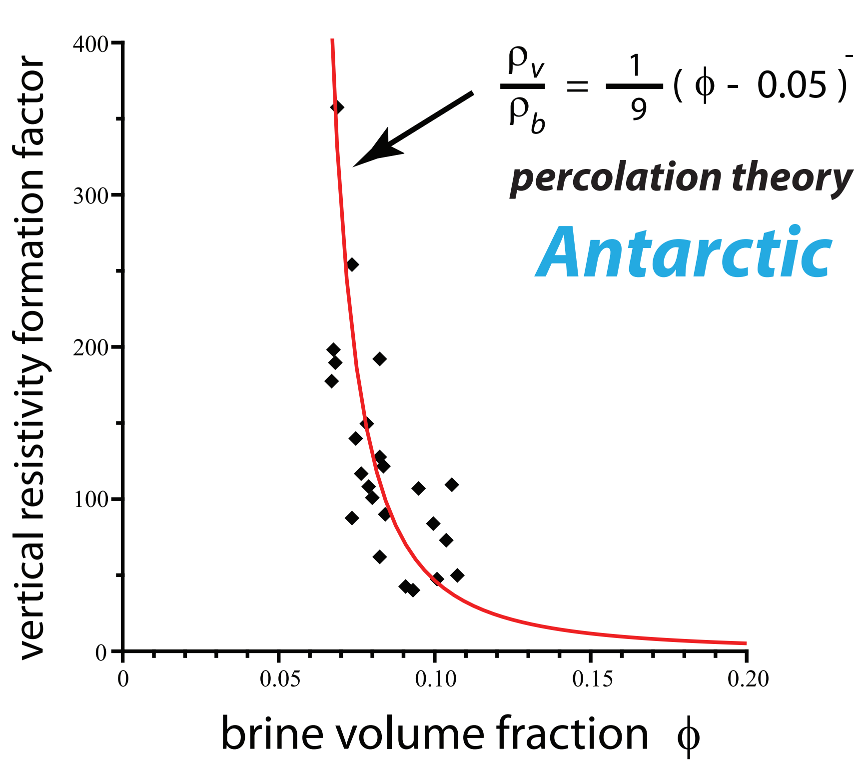

Golden, Eicken, Gully, Ingham, Jones, Lin, Reid, Sampson, Worby 2012

cross borehole tomography

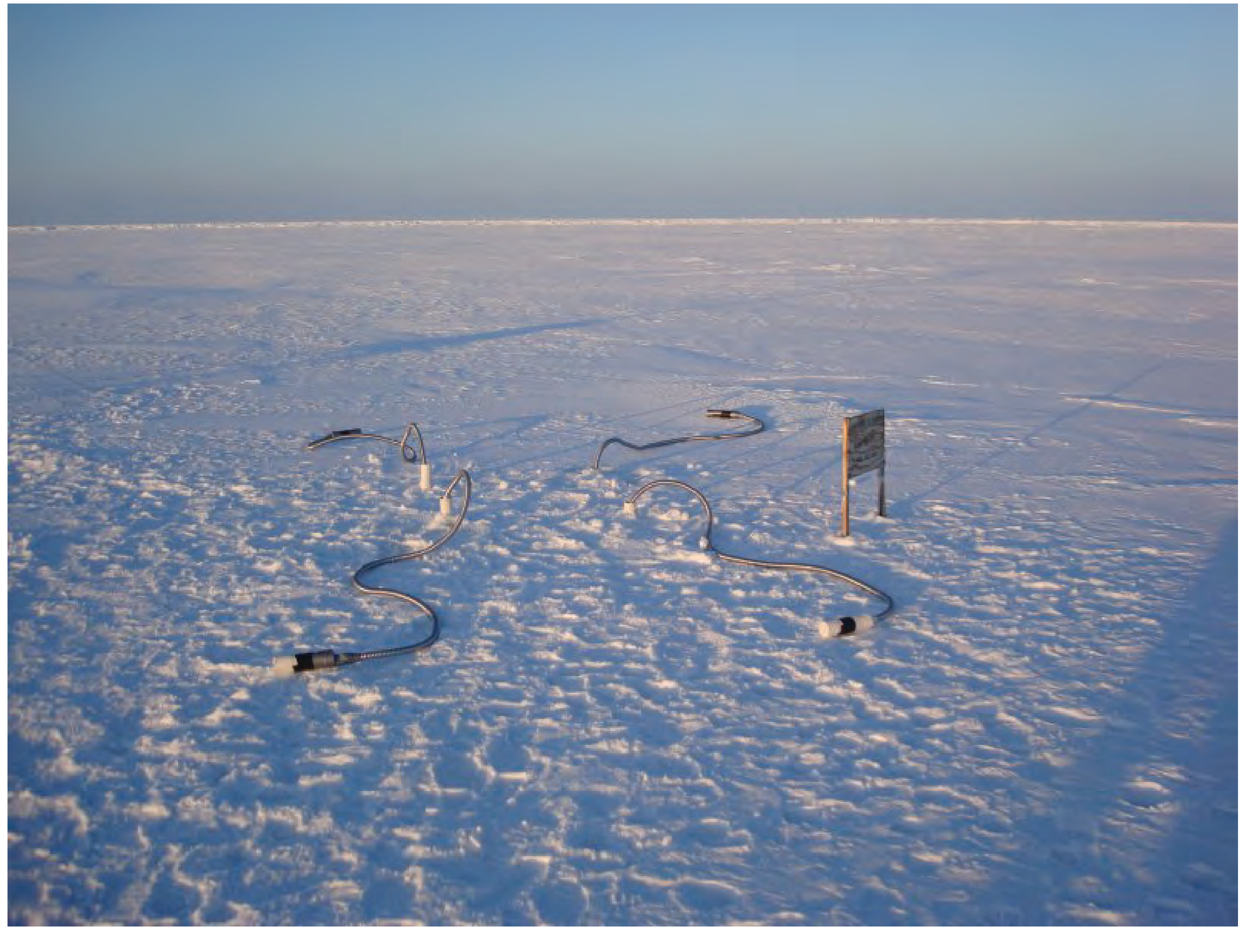

Ingham, Jones, Buchanan
Victoria University, Wellington, NZ

Cross-borehole tomographic reconstructions of the vertical resistivity formation factor for Arctic sea ice before and after melt pond formation

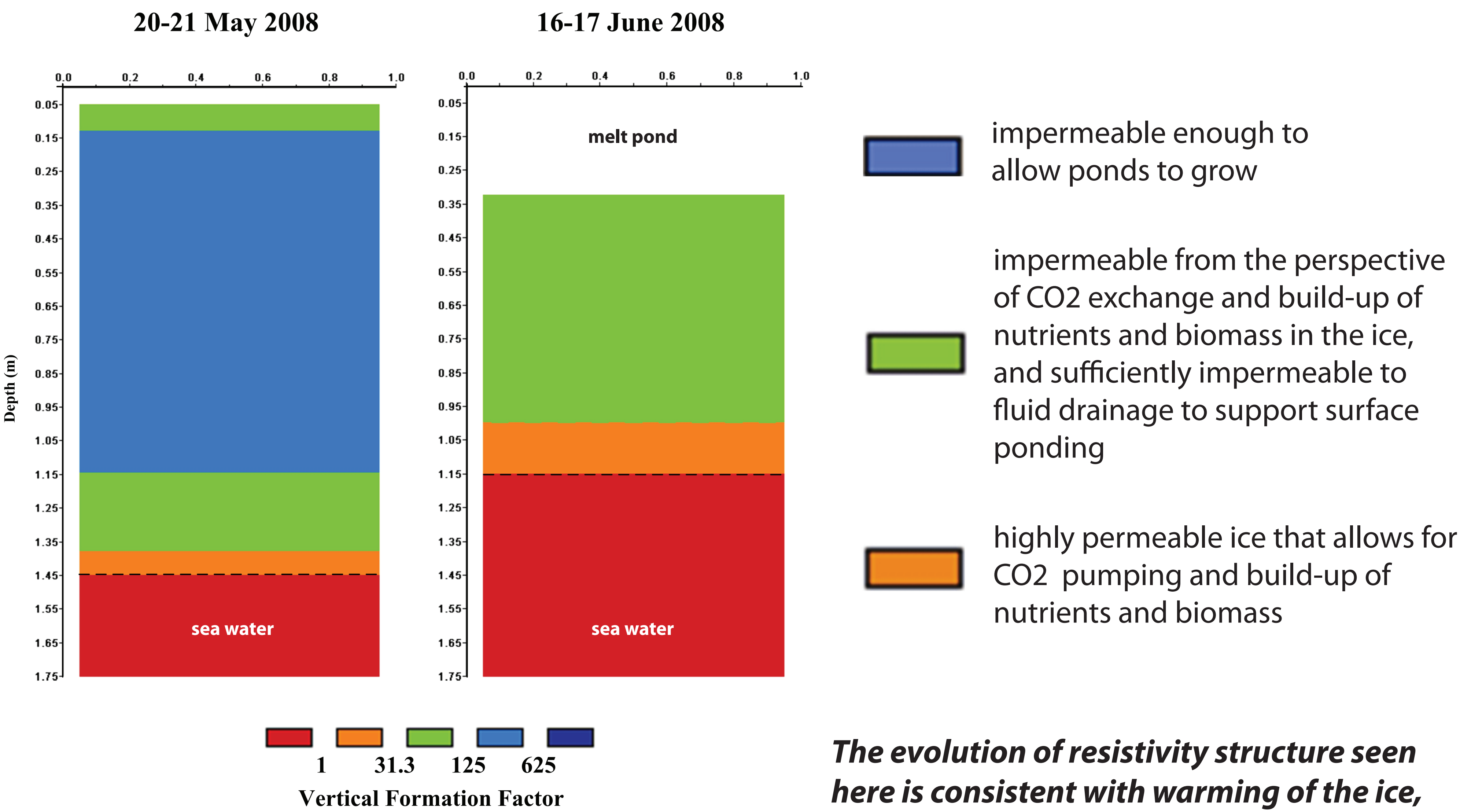

The evolution of resistivity structure seen here is consistent with warming of the ice, thus increasing the fluid permeability.

Golden, Eicken, Gully, Ingham, Jones, Lin, Reid, Sampson, and Worby 2012

multiscale homogenization

Theory of Effective Electromagnetic Behavior of Composites

analytic continuation method

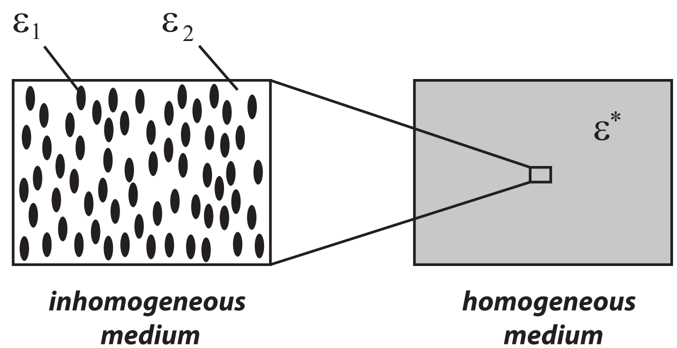

Forward Homogenization Bergman (1978), Milton (1979), Golden and Papanicolaou (1983)

composite geometry **(spectral measure μ)** $\longrightarrow$ ε^*

integral representations, rigorous bounds, approximations, etc.

Inverse Homogenization Cherkaev and Golden (1998), Day and Thorpe (1999), Cherkaev (2001)
(McPhedran, McKenzie, and Milton, 1982)

ε^* $\longrightarrow$ ***composite geometry*** **(spectral measure μ)**

recover brine volume fraction, connectivity, etc.

Effective complex permittivity of a two phase composite in the quasistatic (long wavelength) limit

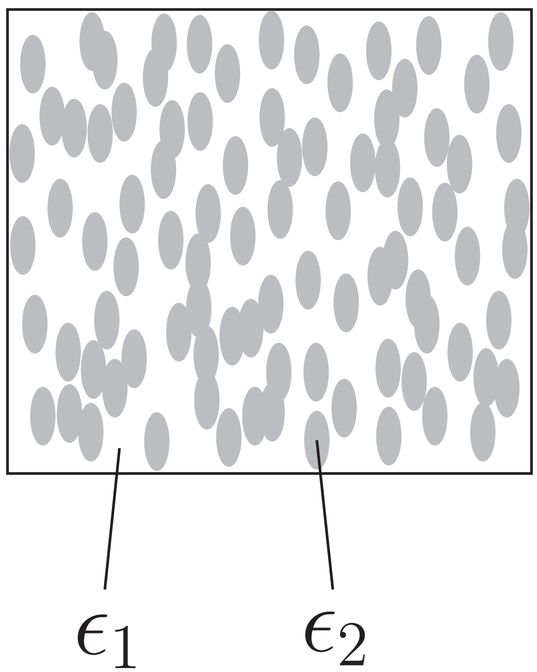

$$\epsilon^*$$

$$D = \epsilon E$$

$$\nabla \cdot D = 0$$

$$\nabla \times E = 0$$

$$\langle D \rangle = \epsilon^* \langle E \rangle$$

p_1 , p_2 = volume fractions of the components

$$\epsilon^* = \epsilon^* \left(\frac{\epsilon_1}{\epsilon_2} \text{ , composite geometry} \right)$$

Stieltjes integral representation

$$F(s) = 1 - \frac{\epsilon^*}{\epsilon_2}, \qquad s = \frac{1}{1 - \epsilon_1 / \epsilon_2}$$

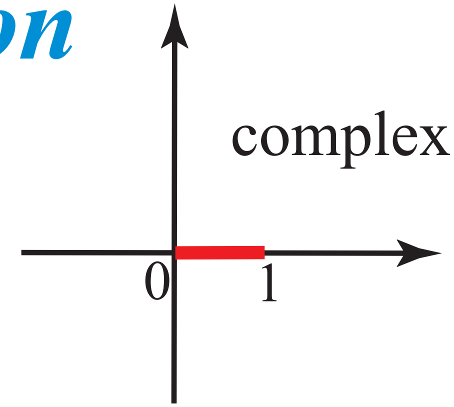

$$F(s) = \int_0^1 \frac{d\mu(z)}{s - z}, \quad \mu$$

- spectral measure of self adjoint operator $\Gamma\chi$
- mass $= p_1$
- higher moments depend on n-point correlations

representation ***separates***

GEOMETRY μ from

medium parameters in s

$$E = (s + \Gamma\chi)^{-1} e_k$$

$$\Gamma = \nabla(-\Delta)^{-1}\nabla \cdot$$

$\chi =$ indicator function of medium 1

forward and inverse bounds for sea ice

matrix particle bounds

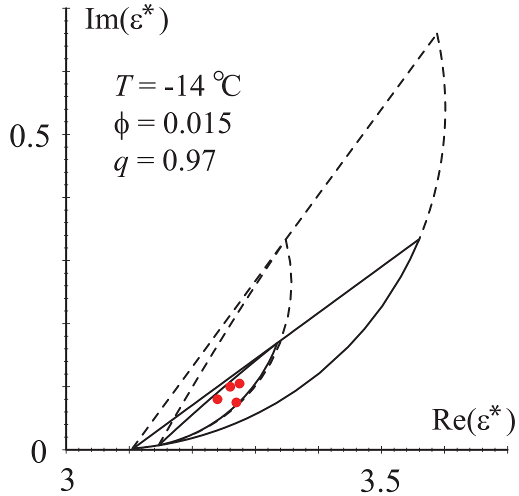

4.75 GHz data

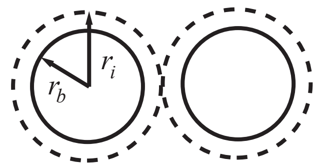

$q = r_b / r_i$

$0 < q < 1$

Golden 1997

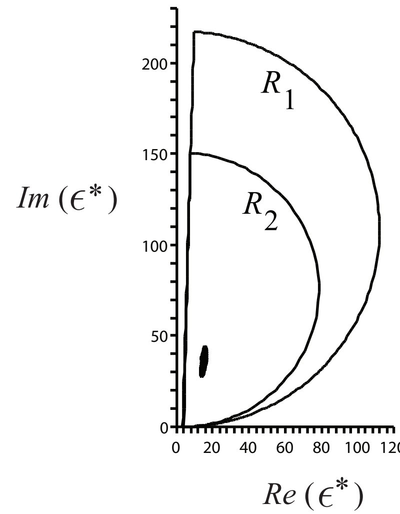

50 MHz capacitance probe data taken near Barrow, AK

inverse bounds and microstructural recovery

Gully, Backstrom, Eicken, Golden, Physica B, 2007

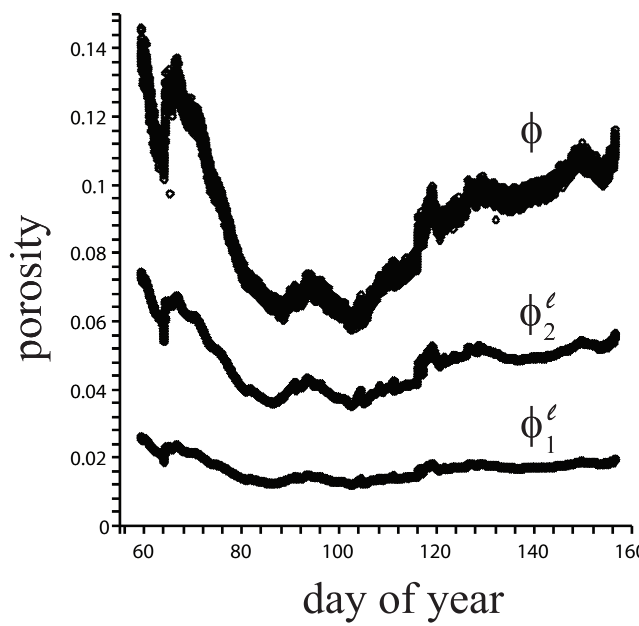

polycrystalline bounds

Gully, Lin, Cherkaev, Golden, 2012

Recovery of inclusion separations in strongly heterogeneous composites from effective property measurements

Chris Orum, Elena Cherkaev, Ken Golden, Proc. Roy. Soc. A, 2012

matrix particle composites (O. Bruno, 1991)

reduced spectral inversion -- construct algebraic curves which bound admissible region in (p,q)-space, q = separation parameter <1

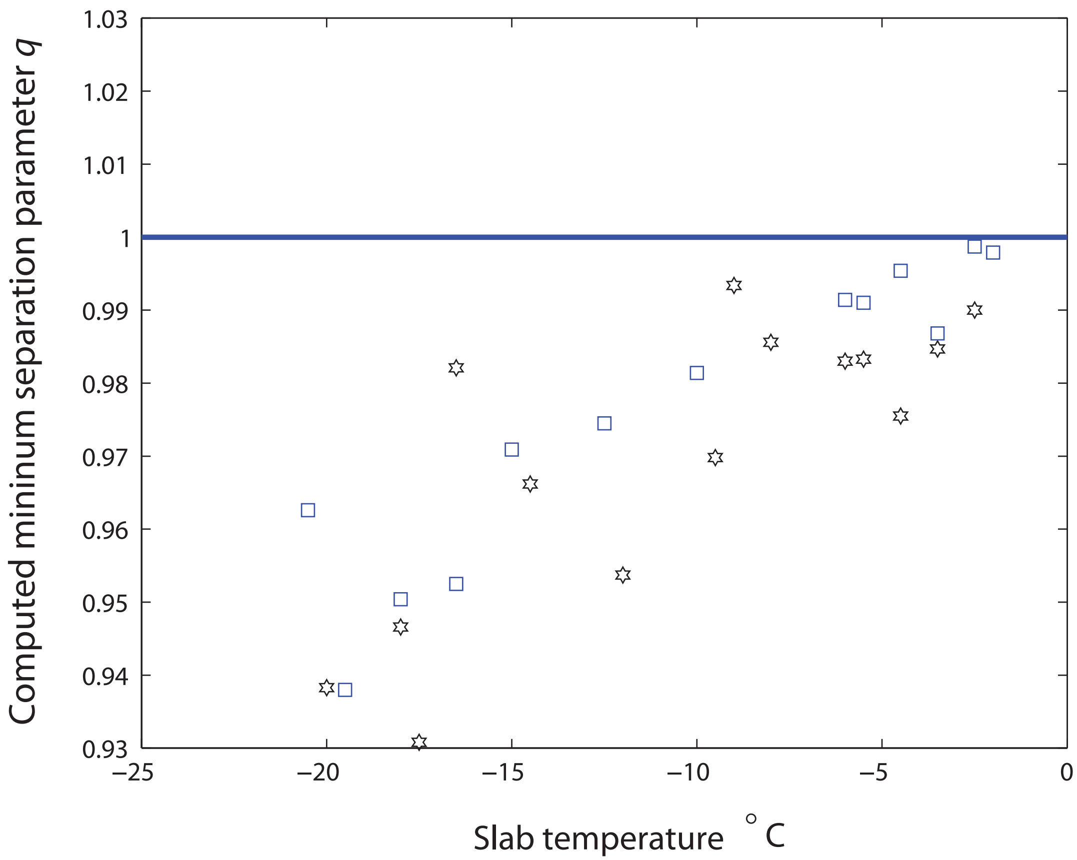

rigorous inverse bound on spectral gap

inversion for brine inclusion separations in sea ice from measurements of effective complex permittivity

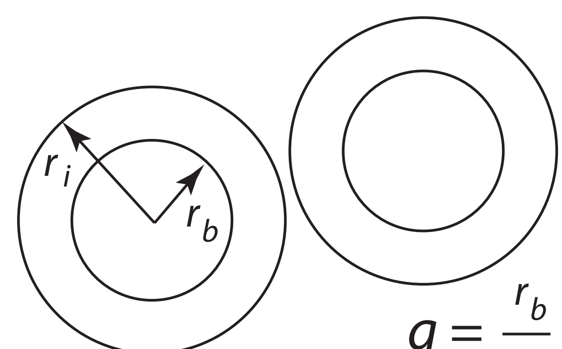

$$q = \frac{r_b}{r_i}$$

Spectral analysis of multiscale sea ice structures

homogenization for brine inclusions, melt ponds, and sea ice pack

how to upscale information on "microstructure"
into effective behavior for larger scales

numerical computation of spectral measure μ

N. B. Murphy, C. Hohenegger, C. S. Sampson, B. Alali, K. Steffen, D. K. Perovich, H. Eicken, and K. M. Golden 2012

spectral measures for 2-d random resistor network

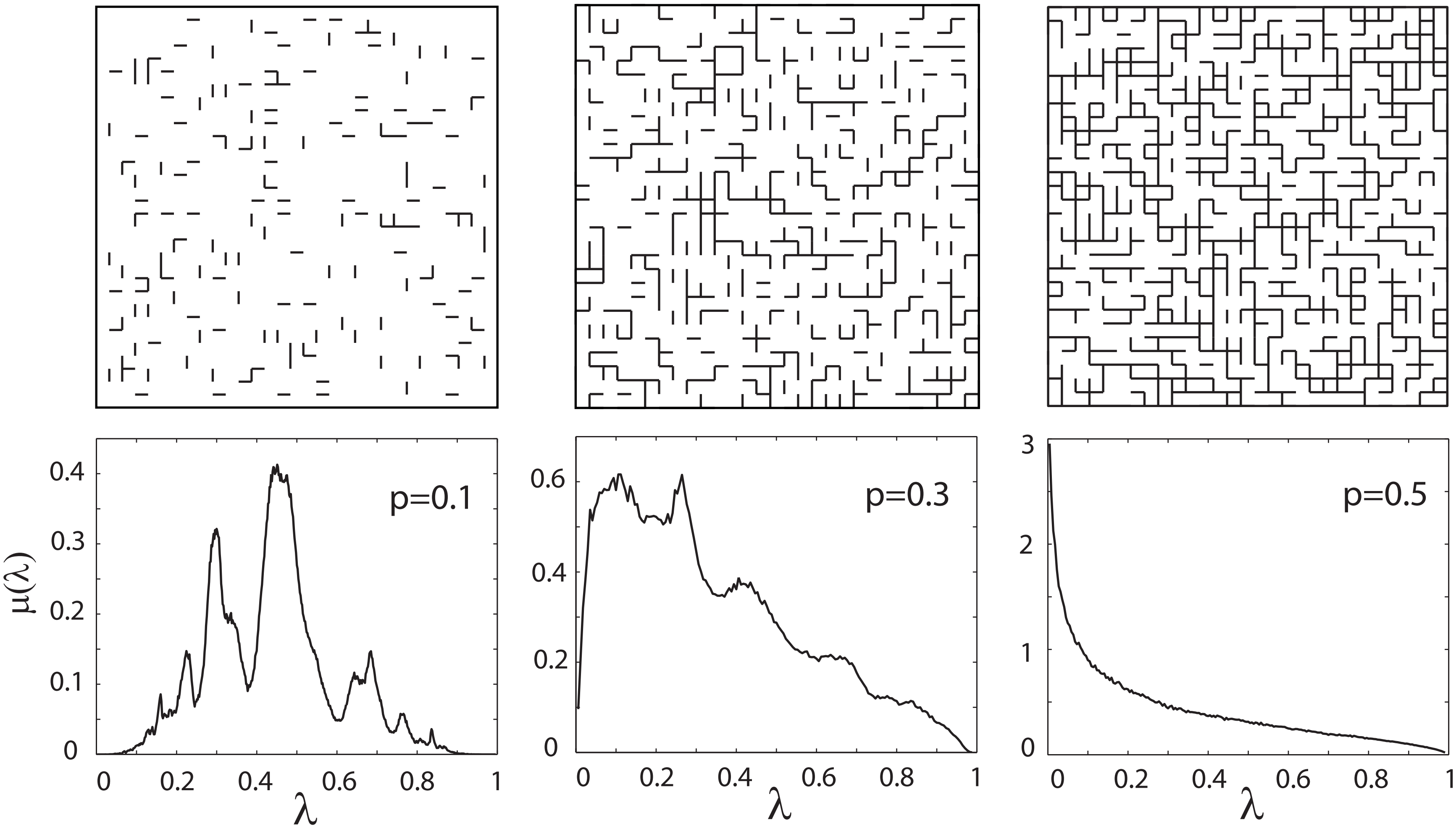

area under curve = p = probability of open bond

spectral gap closes as percolation threshold is approached

random matrix theory calculations of eigenvalue spacing distributions help characterize transitions

spectral measures for Arctic sea ice pack

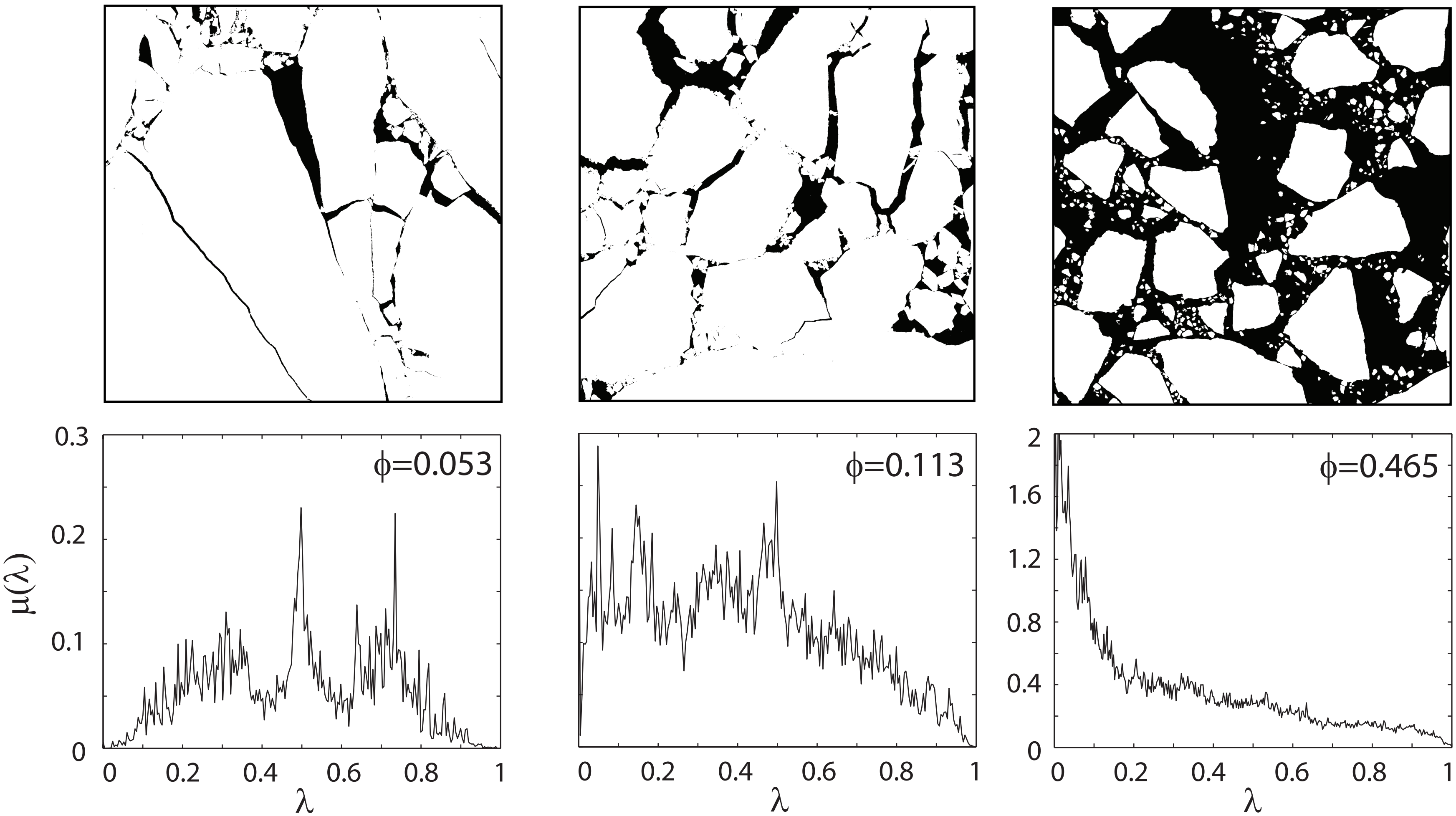

area under curve = ϕ = open water fraction

spectral gap closes as ocean phase becomes connected

advection enhanced diffusion

effective diffusivity

tracers, buoys diffusing in ocean eddies

pollutants

enhanced heat and salt transport

enhanced sea ice thermal conductivity

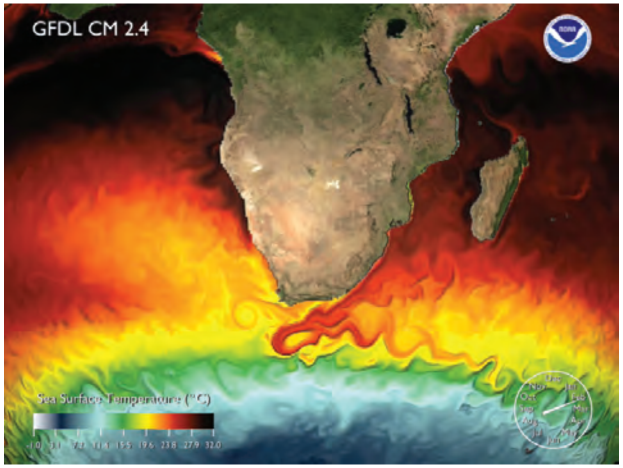

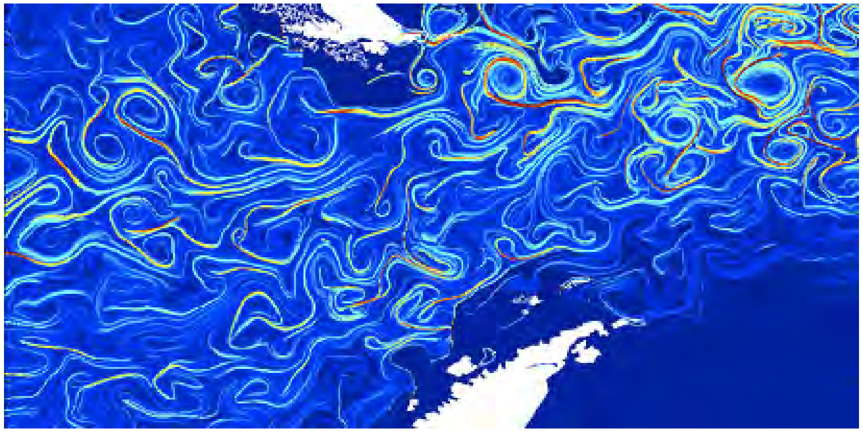

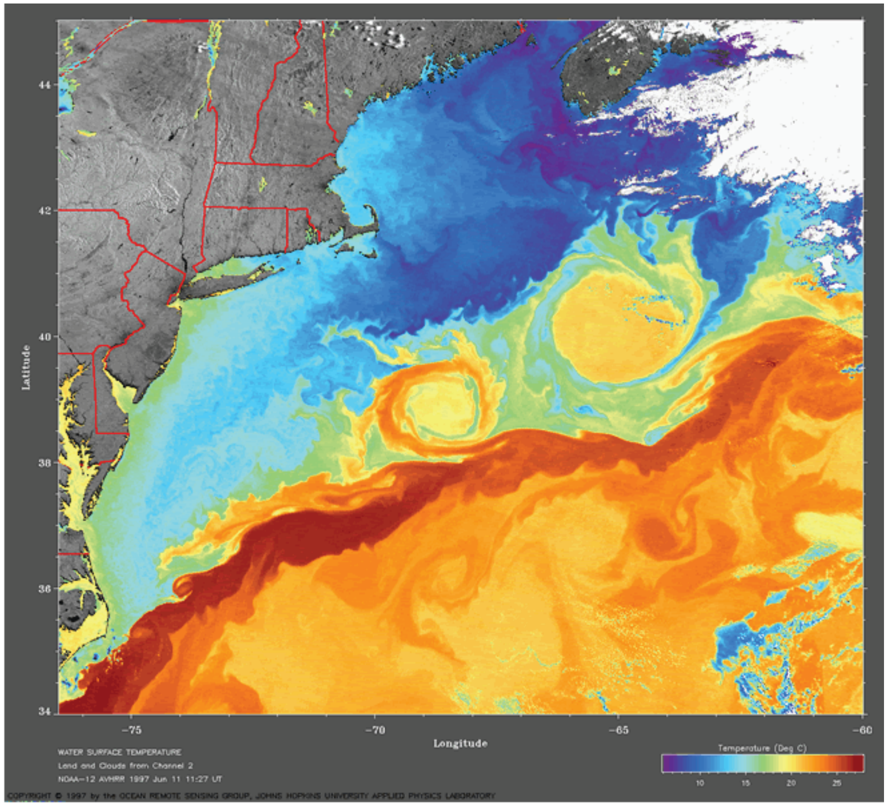

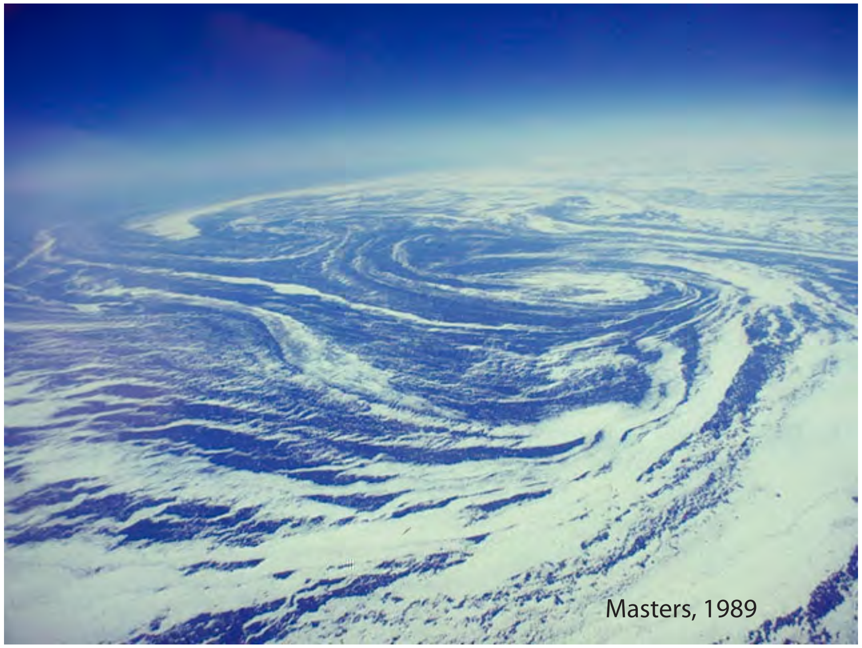

advection diffusion equation with a velocity field u

$$\frac{\partial T}{\partial t} + \mathbf{u} \cdot \nabla T = \kappa_0 \Delta T$$

$$\nabla \cdot \mathbf{u} = 0$$

$\xrightarrow{\textit{homogenize}}$

$$\frac{\partial \overline{T}}{\partial t} = \kappa^* \Delta \overline{T}$$

κ^* effective diffusivity

Stieltjes integral for κ^* with spectral measure

Avellaneda and Majda, PRL 89, CMP 91

composites

$$\frac{\epsilon^*}{\epsilon_2} = 1 - \int_0^1 \frac{d\mu(z)}{s - z}$$

$$s = \frac{1}{1 - \epsilon_1 / \epsilon_2}$$

μ spectral measure of $\Gamma\chi$

advection diffusion

$$\frac{\kappa^*}{\kappa_0} = 1 - \int_0^\infty \frac{d\rho(z)}{t - z}$$

ξ = Péclet number $\quad t = -1/\xi^2$

ρ spectral measure of $\Gamma \mathbf{H}$

$\mathbf{u} = \nabla \cdot \mathbf{H} \quad \mathbf{H}$ antisymmetric vector potential

spectral calculations for sample vortices

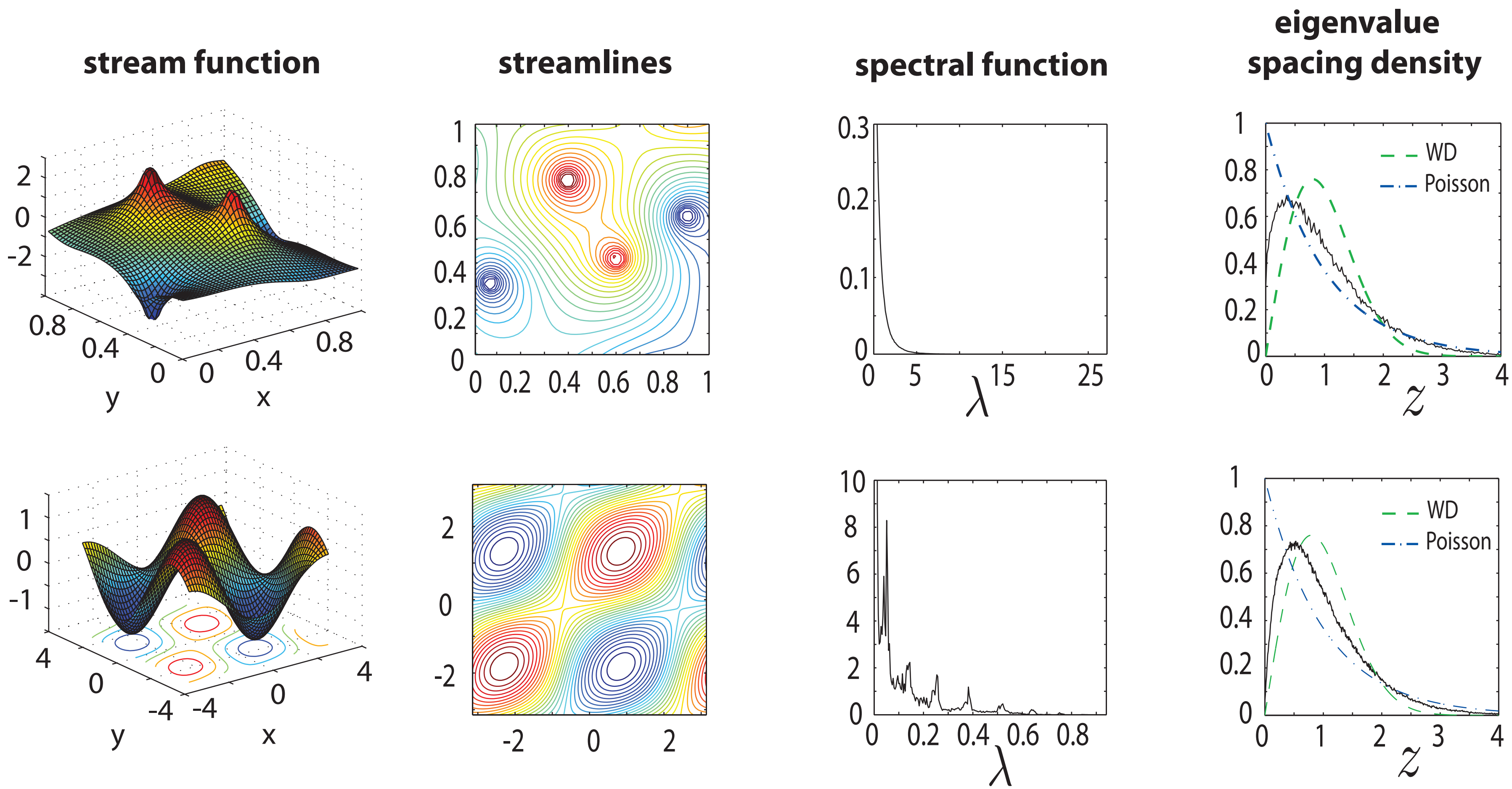

Murphy, Zhu, Golden, 2012

convection enhanced thermal conductivity of sea ice for shear flow

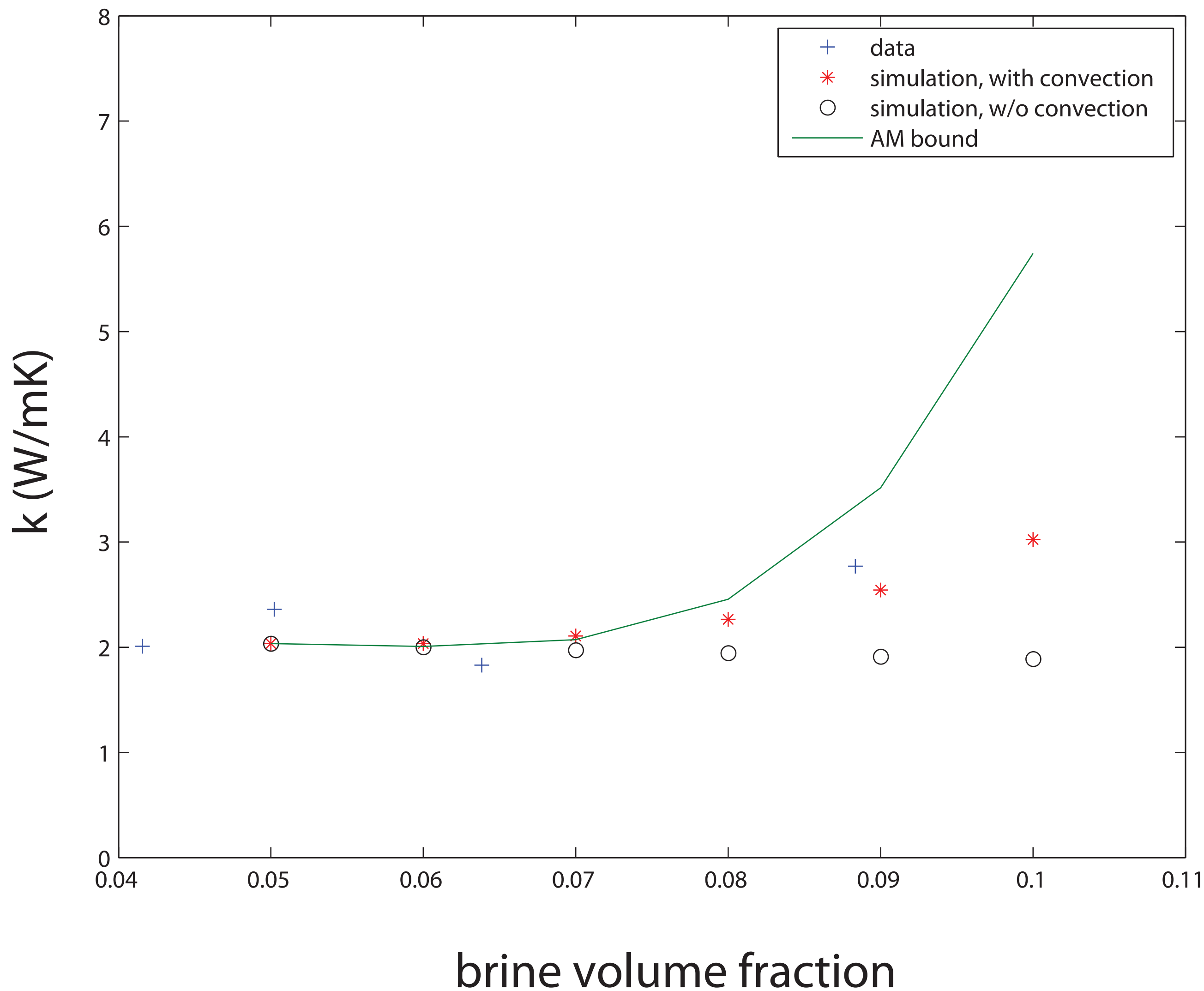

Wang, Zhu, Golden, 2012

fractals and multiscale structure

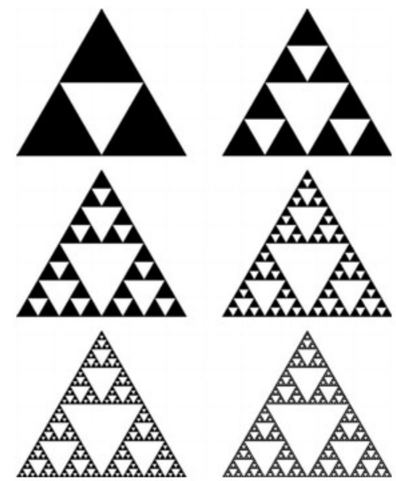

sea ice displays ***multiscale*** structure over 10 orders of magnitude

0.1 millimeter

1 meter

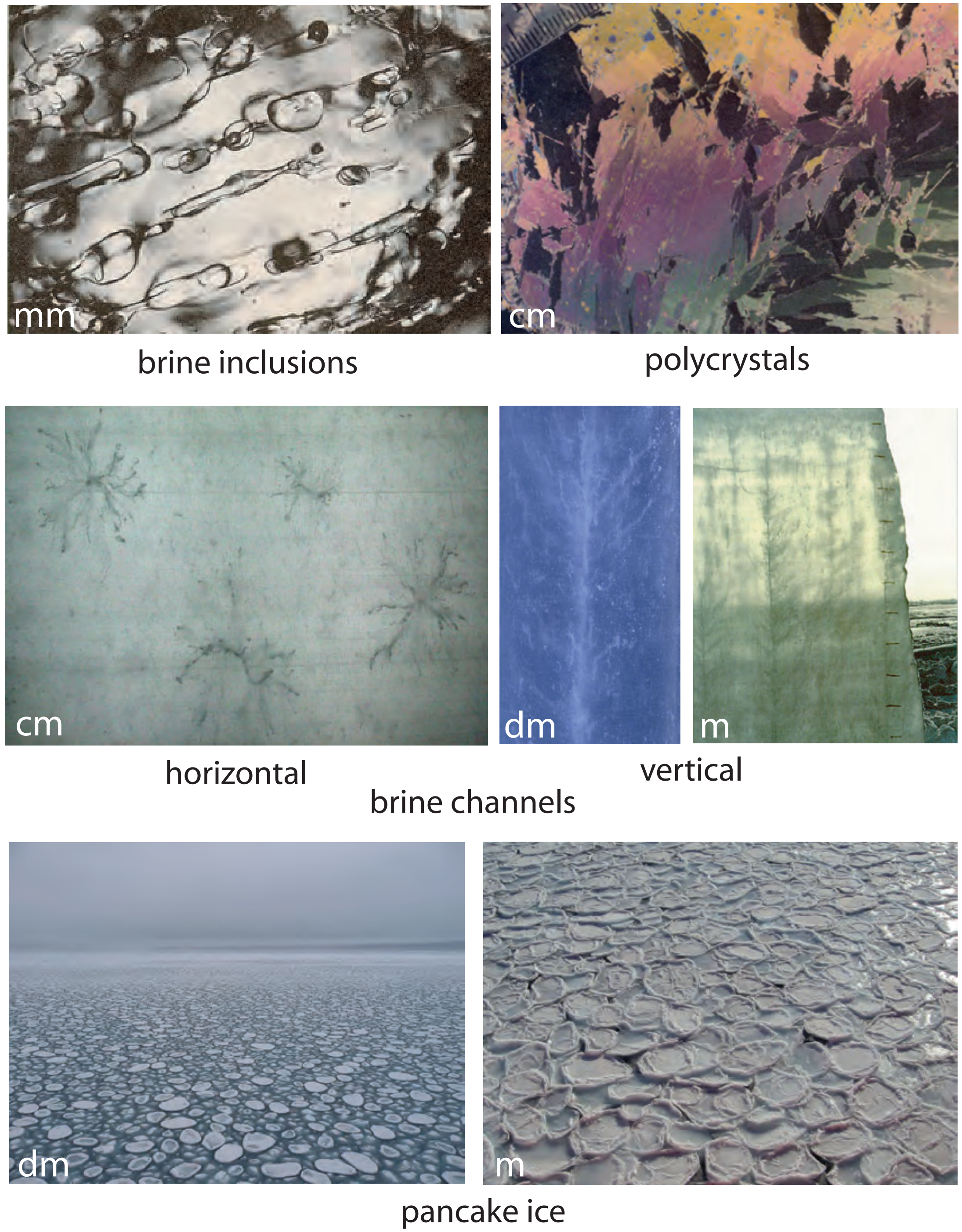

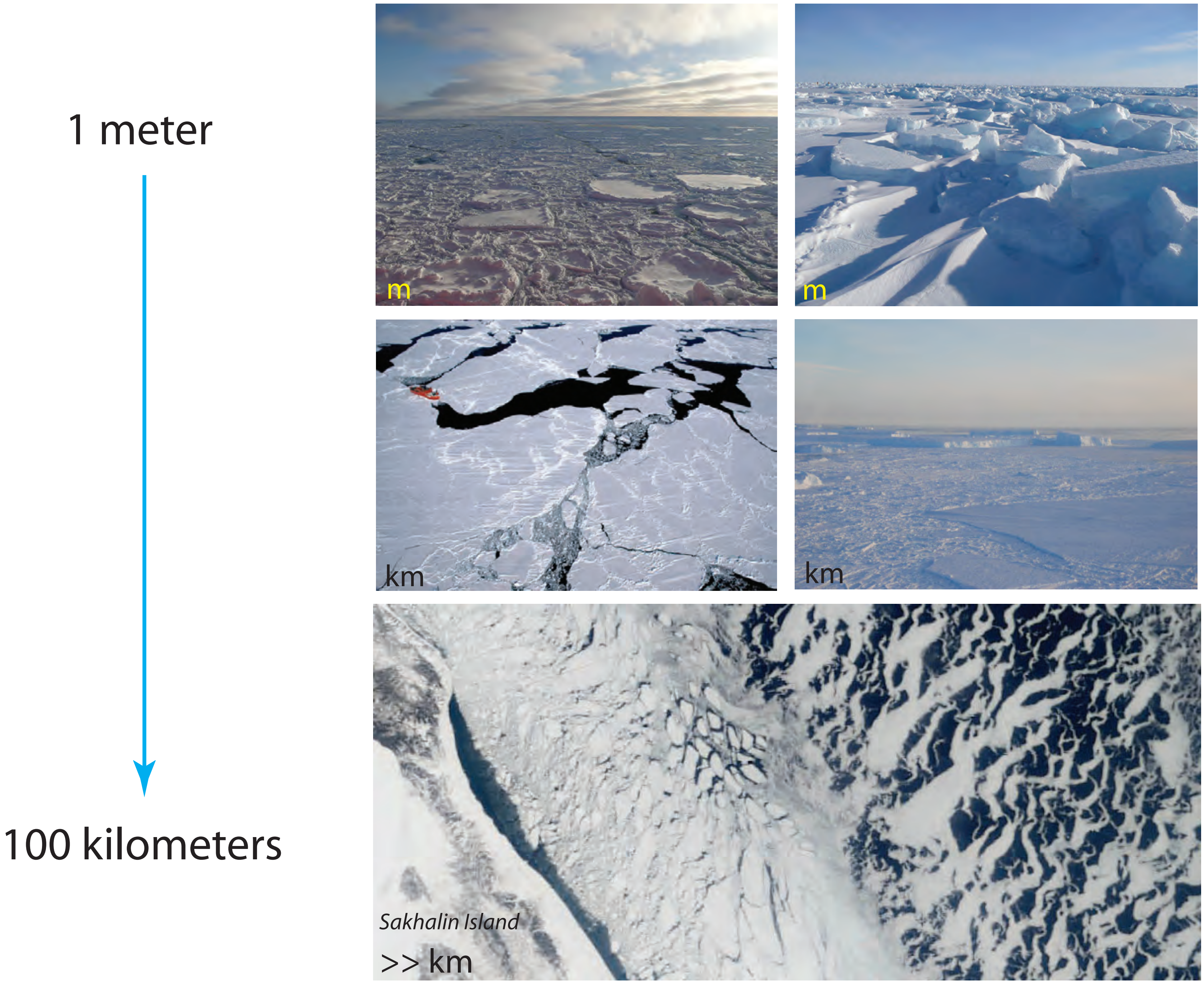
1 meter
100 kilometers
m
m
km
km
Sakhalin Island
>> km

melt pond formation and albedo evolution:

- major drivers in polar climate
- key challenge for global climate models

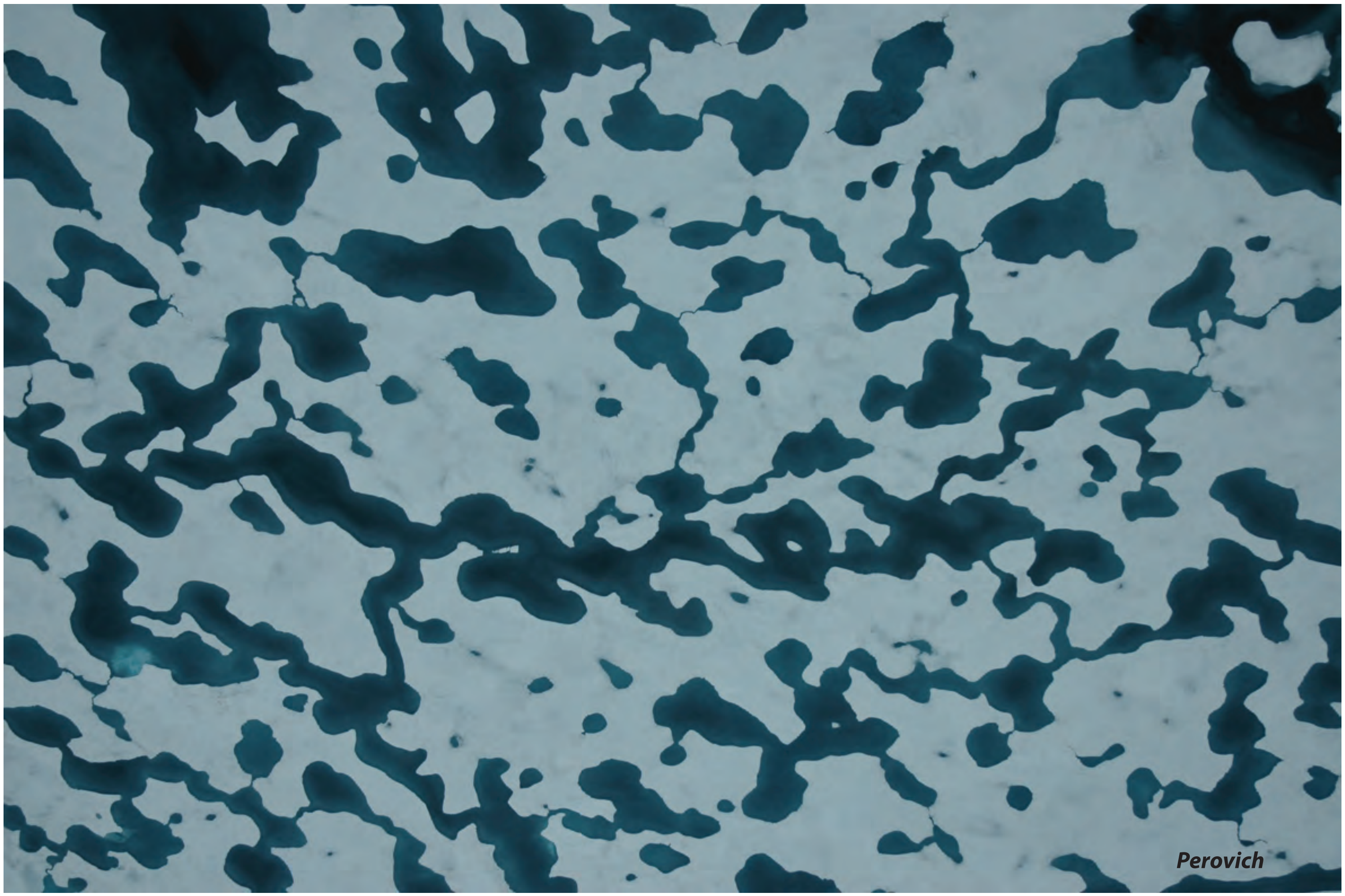

Do melt ponds exhibit interesting multiscale structure?

Are there universal features of the evolution similar to phase transitions in statistical mechanics?

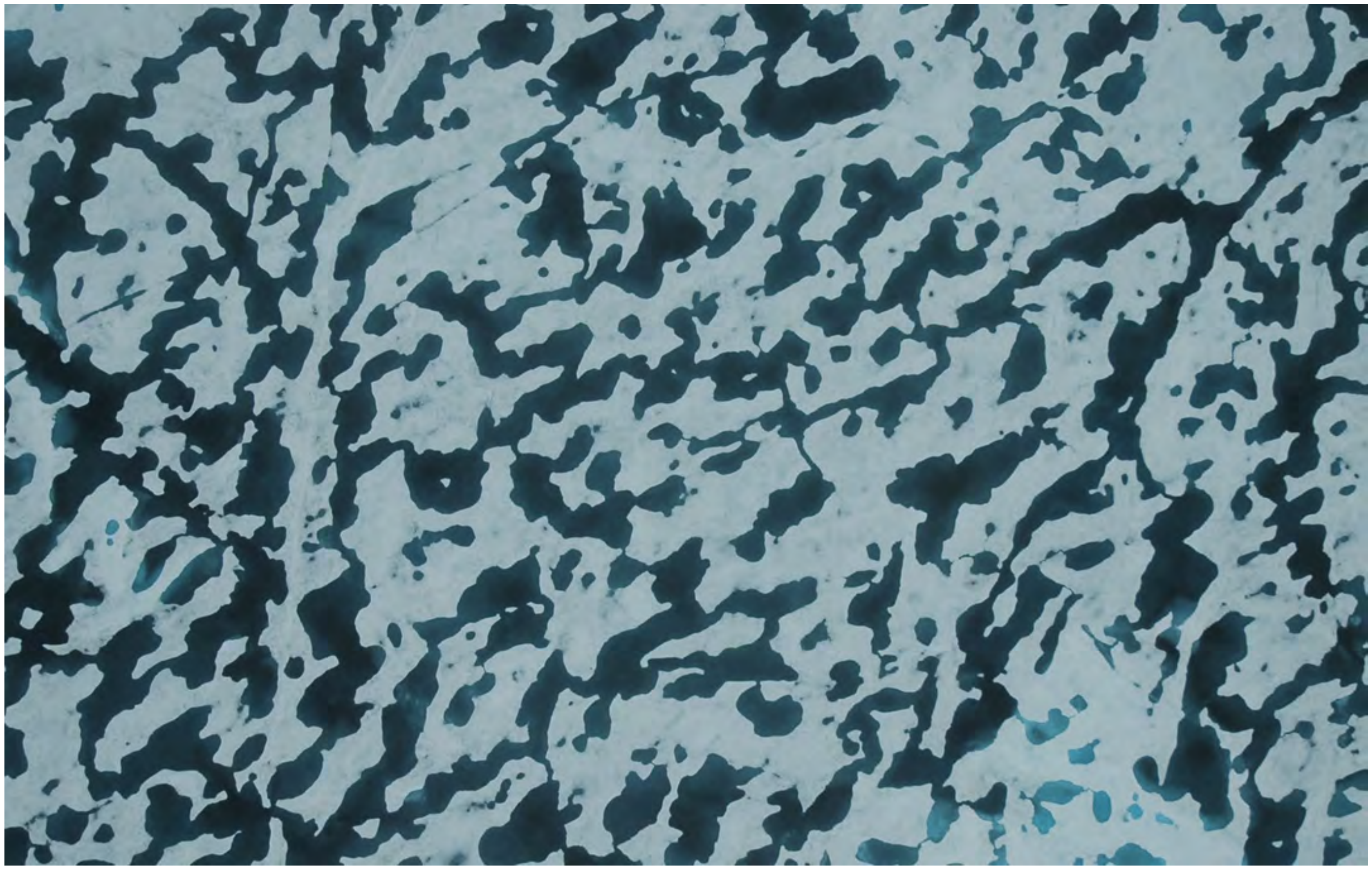

Transition in the fractal geometry of Arctic melt ponds

Christel Hohenegger, Bacim Alali, Kyle Steffen, Don Perovich, Ken Golden

fractal curves in the plane

they wiggle so much that their dimension is >1

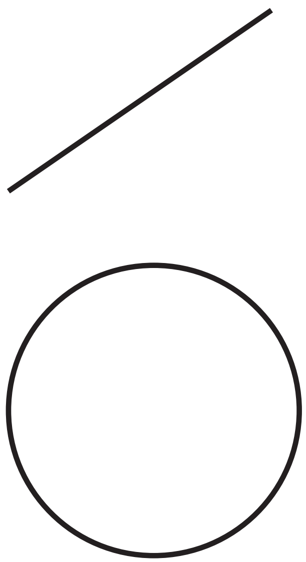

simple curves

$D = 1$

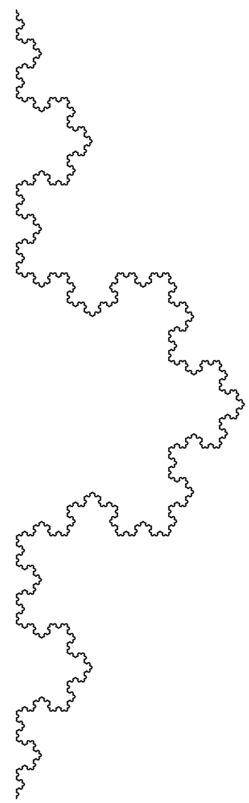

Koch snowflake

$D = 1.26$

Peano curve

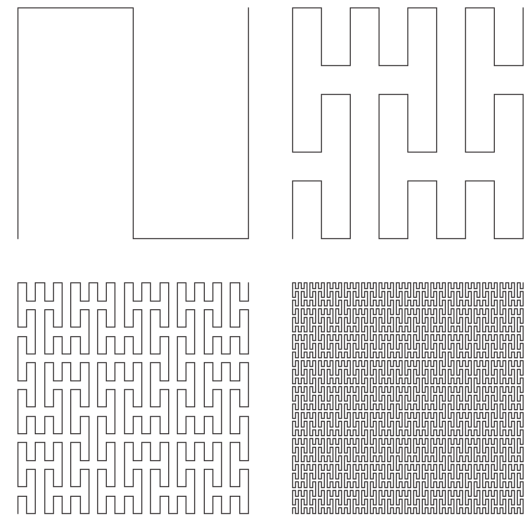

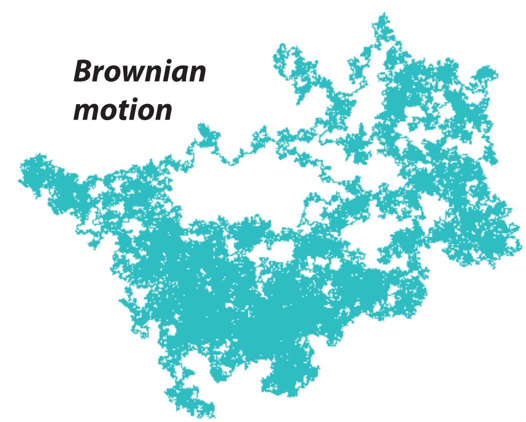

space filling curves

$D = 2$

clouds exhibit fractal behavior from 1 to 1000 km

use ***perimeter-area*** data to find that cloud and rain boundaries are fractals

$$D \approx 1.35$$

S. Lovejoy, Science, 1982

$$P \sim \sqrt{A}$$

simple shapes

L

L

$A = L^2$

$P = 4L = 4\sqrt{A}$

$$P \sim \sqrt{A}^{\,D}$$

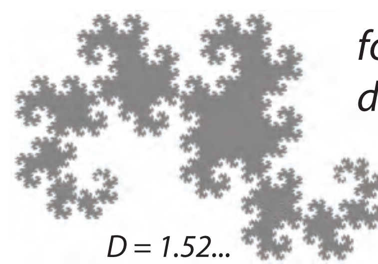

for fractals with dimension D

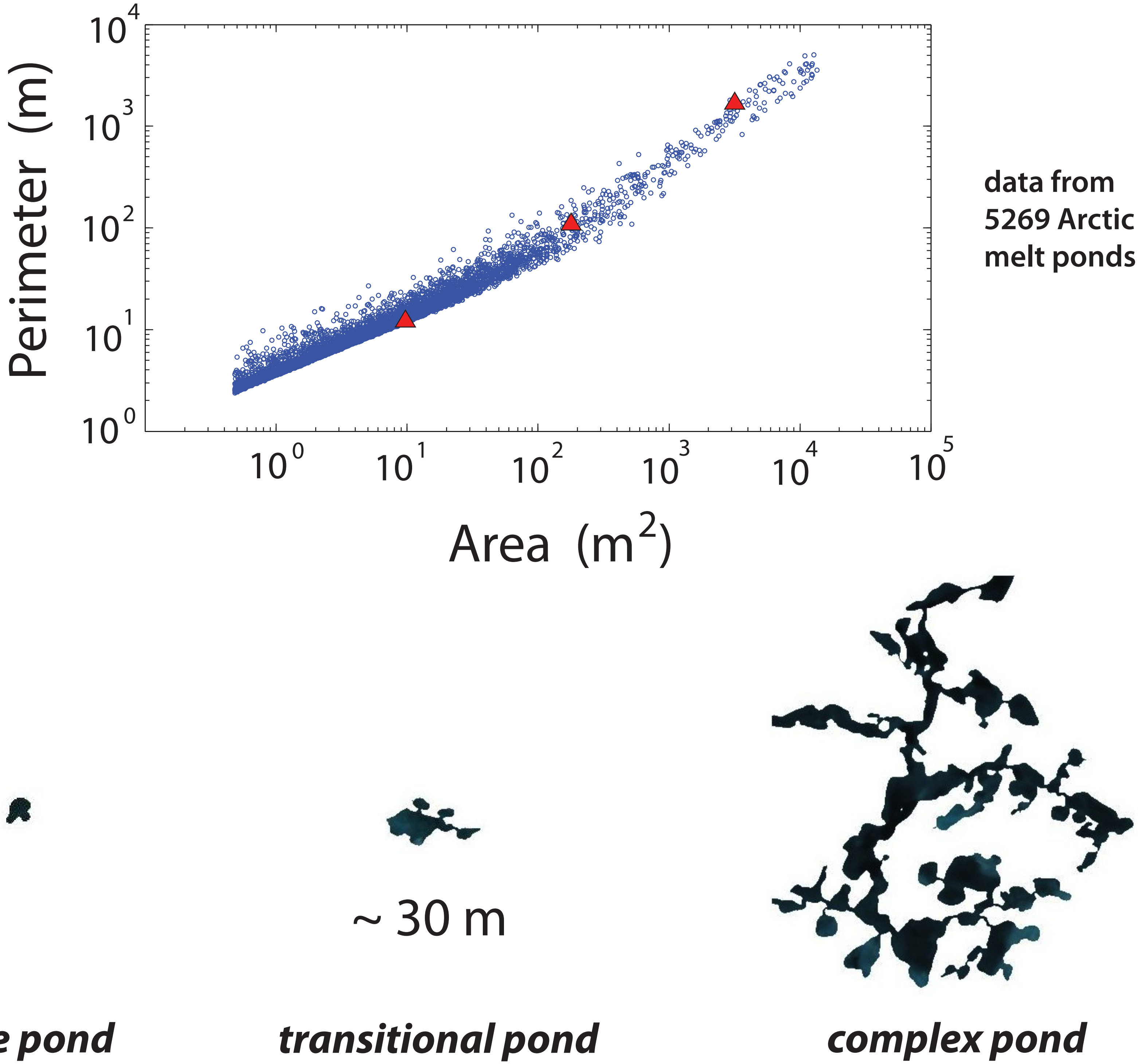
Perimeter (m)
Area (m^2)
10^0
10^1
10^2
10^3
10^4
10^5
data from
5269 Arctic
melt ponds
~ 30 m
simple pond
transitional pond
complex pond

transition in the fractal dimension

complexity grows with length scale

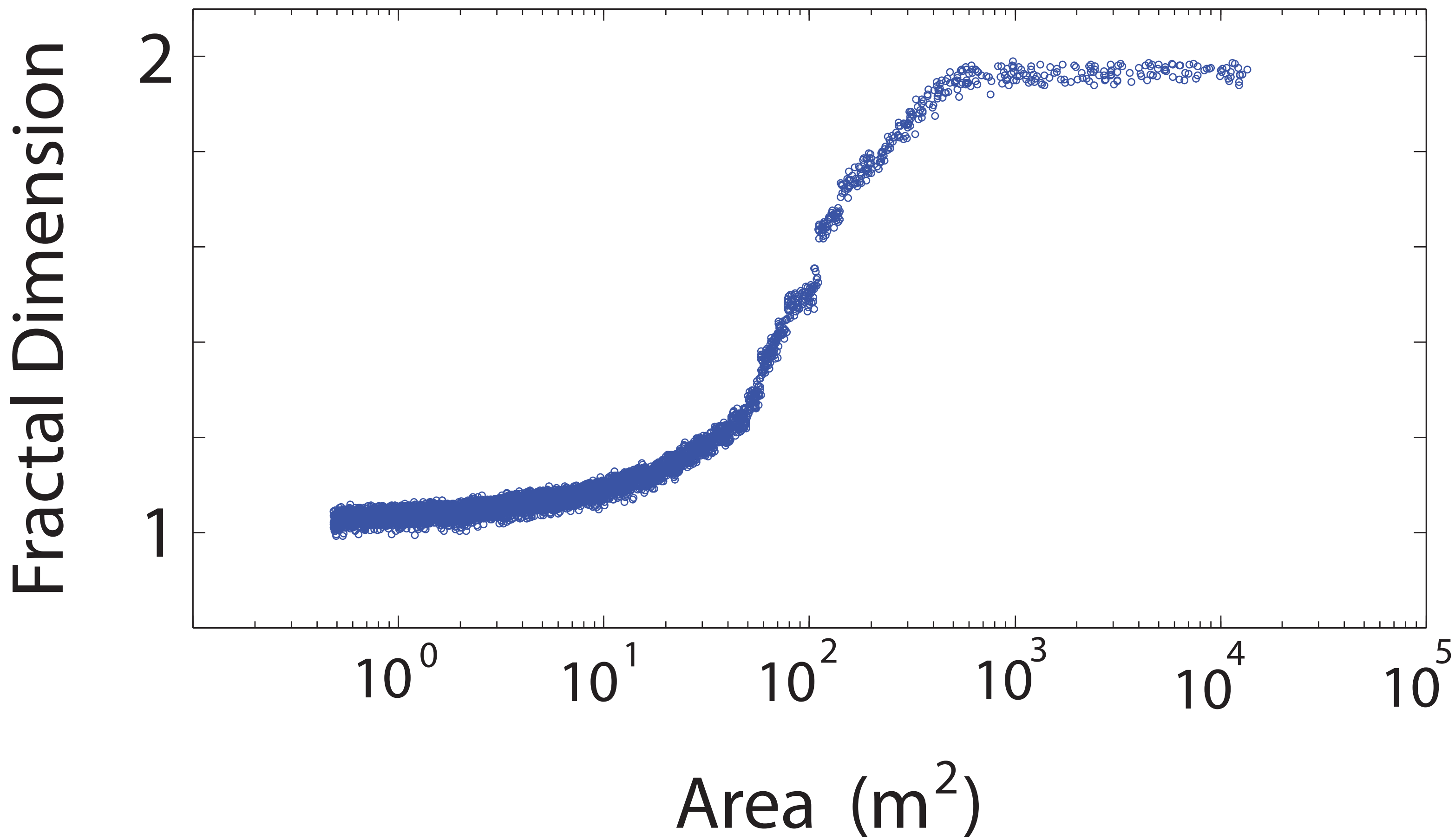

compute “derivative” of area - perimeter data

small simple ponds coalesce to form
large connected structures with complex boundaries

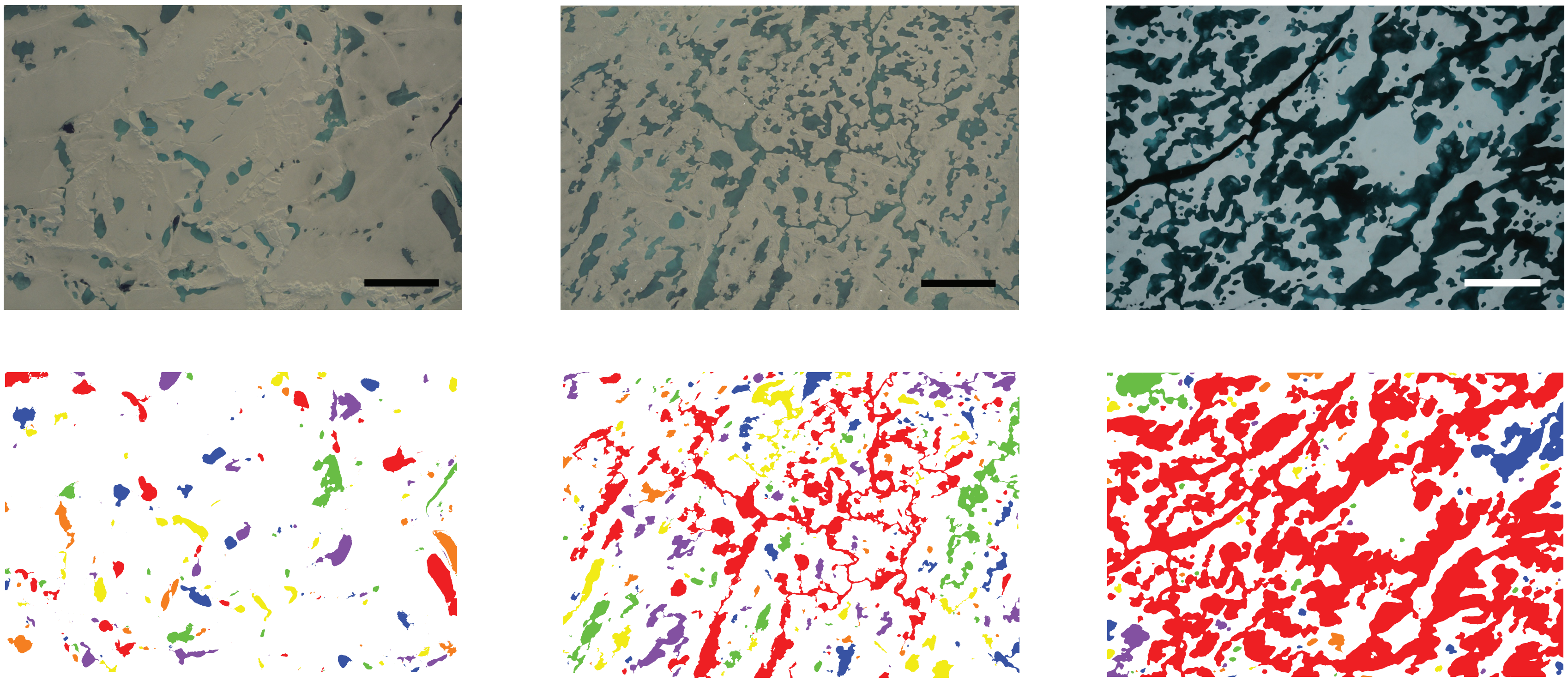

melt pond percolation

Buchanan Bay, Antarctica Mertz Glacier Polynya Experiment July 1999